Research Square

Preprints are preliminary reports that have not undergone peer review.
They should not be considered conclusive, used to inform clinical practice,
or referenced by the media as validated information.

# Metal–1,10-Phenanthroline-5,6-dione Complexes Target Multidrug-Resistant Acinetobacter baumannii: Antibacterial and Pharmacodynamic Insights

**Ingrid Peregrino**
Universidade Federal do Espírito Santo
**Gabriela Seabra**
Universidade Federal do Espírito Santo
**Luiz Felipe Santos**
Universidade Federal do Espírito Santo
**Roberta Mendes**
Universidade Federal do Espírito Santo
**Michael Devereux**
Technological University Dublin
**Malachy McCann**
National University of Ireland, Maynooth
**Lívia Ramos**
Universidade Federal do Rio de Janeiro
**André Santos**
andre@micro.ufrj.br

Universidade Federal do Rio de Janeiro
**Ana Paula Nunes**
Universidade Federal do Espírito Santo

**Research Article**

**Keywords:** Ag-phendione, antimicrobial resistance, Acinetobacter baumannii, Cu-phendione, pharmacodynamics

**Posted Date:** September 12th, 2026

**DOI:** https://doi.org/10.21203/rs.3.rs-10922740/v1

**License:** This work is licensed under a Creative Commons Attribution 4.0 International License.
Read Full License

**Additional Declarations:** No competing interests reported.

# Abstract

The escalating threat of antimicrobial resistance underscores the need for novel therapeutic strategies against multidrug-resistant (MDR) Gram-negative pathogens. We previously demonstrated the potent antimicrobial activity of 1,10-phenanthroline-5,6-dione (phendione) complexes with silver(I) (Ag-phendione) and copper(II) (Cu-phendione) against MDR *Acinetobacter baumannii*. Herein, we further characterized the antibacterial activity and pharmacodynamic profiles of these complexes against six MDR clinical isolates and the reference strain ATCC19606. Exposure-response relationships, dose-fractionation regimens, post-antibiotic effects (PAEs) and the influence of bacterial inoculum on minimum inhibitory concentrations (MICs) were investigated. Potential interactions with meropenem and imipenem were assessed by checkerboard and time-kill assays, while recalcitrance was evaluated by modified disk-diffusion assays. Ag-phendione consistently exhibited bactericidal activity, whereas Cu-phendione displayed either bactericidal or bacteriostatic effects depending on the strain. Ag-phendione demonstrated greater antibacterial potency and predominantly time-dependent activity, with maximal effects observed between 6 and 12 h. Notably, dose fractionation with two administrations of 0.5×MIC at 6-h intervals maintained sustained bactericidal activity, resulting in complete eradication of all tested isolates within 24 h. MICs remained unchanged across different inoculum sizes, indicating robust activity under varying bacterial burdens. At 3.12 μg/mL, both complexes reduced bacterial populations by more than 97%. Ag-phendione produced a substantially longer PAE than Cu-phendione (1.857 versus 0.714 h). Combination assays with meropenem and imipenem predominantly showed additive interactions accompanied by significant reductions in bacterial burden. Importantly, neither complex induced detectable tolerance or heteroresistance under the conditions tested. Collectively, phendione complexes show promising antimicrobial and pharmacodynamic activity against MDR *A. baumannii*, warranting further investigation as therapeutic candidates.


# Introduction

The escalating problem of antimicrobial resistance (AMR) has led to a critical shortage of effective therapeutic options, particularly against multidrug-resistant (MDR) bacterial infections, which represent a significant challenge for clinicians and a serious threat to human health (Baran et al. 2023). In 2021, bacterial AMR was associated with an estimated 4.71 million deaths, including 1.14 million directly attributable to it (GBD 2021). Furthermore, resistance to carbapenems increased more than any other antibiotic class among Gram-negative bacteria, rising from 619.000 associated and 127.000 attributable deaths in 1990, to 1.03 million associated and 216.000 attributable deaths in 2021 (GBD 2021). In this context, carbapenem-resistant *Acinetobacter baumannii* (CRAb) is particularly notorious for causing severe infections in healthcare settings, which are associated with high mortality rates (Cavallo et al. 2023; Mancuso et al. 2023; Li et al. 2024). The World Health Organization (WHO) has placed CRAb in the highest priority category for research and development of new antibiotics, highlighting the urgent need for innovative therapeutic alternatives (WHO 2017, 2024). Currently, researchers are actively exploring new strategies to combat these critical pathogens, aiming to overcome the limitations of existing

treatments and mitigate the impact of AMR on public health (Gupta and Sharma 2022; MacNair et al. 2023).

In response to the rapid rise of AMR and the challenges associated with developing antibiotics with novel mechanisms of action, coordination compounds (or complexes) have garnered interest as promising alternatives to conventional antibiotics (Claudel et al. 2020; Evans and Kavanagh 2021; O'Shaughnessy et al. 2022; Frei et al. 2023; Rakshit et al. 2023). Central to this field are 1,10-phenanthroline (phen) and its derivative 1,10-phenanthroline-5,6-dione (phendione), known for their unique structural features and remarkable ability to form stable complexes with transition metals (Viganor et al. 2017). Several of these metal–ligand complexes have demonstrated potent antimicrobial activity against bacteria, fungi and parasites, positioning them as promising alternatives to conventional antimicrobial agents (Viganor et al. 2016; Mohan and Choudhary 2021; O'Shaughnessy et al. 2022; Oliveira et al. 2023; Gandra et al. 2024). The antimicrobial activity of phen/phendione-based complexes is primarily attributed to their capacity to generate reactive oxygen species, which induce oxidative damage to key cellular components (McCann et al. 2004; Viganor et al. 2017; Galdino et al. 2022; Sousa et al. 2023; Frota et al. 2024). In this context, our research group has explored the antimicrobial potential of $[Cu(phendione)_3](ClO_4)_2 \cdot 4H_2O$ (Cu-phendione) and $[Ag(phendione)_2]ClO_4$ (Ag-phendione) complexes, demonstrating promising activity against clinical strains of *P. aeruginosa* (Viganor et al. 2016), *A. baumannii* (Ventura et al. 2020), and *Klebsiella pneumoniae* (Peregrino et al. 2021). Moreover, in silico analyses have predicted favorable pharmacokinetic profiles for both complexes (Giovanini et al. 2025). Consistent with these predictions, cytotoxicity studies have demonstrated that Ag-phendione and Cu-phendione are well tolerated in vitro across a range of mammalian cell lines and in vivo in multiple experimental models, including *Galleria mellonella* larvae (McCann et al. 2012), Swiss mice (McCann et al. 2012), and golden hamsters (Santos et al. 2022). This biocompatibility, combined with their potent antimicrobial activity, highlights their strong potential as therapeutic agents for further preclinical and clinical development.

Assessing the pharmacodynamic (PD) profile of an antimicrobial candidate early in development is crucial for understanding its action, optimizing therapeutic outcomes and mitigating resistance risks (Mozhayskiy and Tagkopoulos 2013). Nonclinical PD experiments that elucidate the time-course of antimicrobial effects and the pattern of bacterial killing/regrowth provide a more comprehensive understanding of the compound's therapeutic potential beyond traditional minimum inhibitory concentration (MIC) measurements (Rodríguez-Gascón and Solinís 2021; Minichmayr et al. 2022). While MIC is a valuable indicator of antimicrobial potency, it has limitations due to its static concentration conditions, which do not reflect the dynamic in vivo environment (Yu et al. 2019; Van and Zeitlinger 2021). Therefore, more advanced PD assessments are necessary to determine antimicrobial activity profiles (bacteriostatic versus bactericidal; concentration-dependent versus time-dependent), bacterial killing rates and duration of post-antibiotic effects when concentrations fall below the MIC (Lister 2006; Rodríguez-Gascón and Solinís 2021). Summarily, early PD evaluations play a pivotal role in identifying the parameters influencing clinical efficacy, setting optimal regimens for achieving maximum therapeutic

effect, and ensuring the best conditions for subsequent clinical trials (Jorda and Zeitlinger 2020; Palmer et al. 2022; Bissantz et al. 2024).

Building on these premises, this study aims to characterize the PD profile of Cu-phendione and Ag-phendione against MDR *A. baumannii* strains. To achieve this, exposure–response curve analyses, dose-fractionation studies, post-antibiotic effect (PAE) determination, and MIC determination varying the inoculum size were performed. Additionally, we sought to further assess the antimicrobial efficacy of these complexes through synergy assays with carbapenems, including checkerboard and time-kill experiments, and to investigate their potential to induce bacterial recalcitrance. By advancing our understanding of these promising novel agents, we aim to contribute to the development of innovative therapeutic strategies to treat infections caused by MDR *A. baumannii*.

## Materials and Methods

# Test compounds

The phendione-based complexes, Cu-phendione and Ag-phendione, were prepared following published methods (McCann et al. 2004). The compounds were dissolved in dimethyl sulfoxide and stored at 4ºC in the dark. Meropenem (MEM - Sigma-Aldrich), imipenem (IMP - Sigma-Aldrich) and ciprofloxacin (CIP - Sigma-Aldrich) were dissolved in sterile water and stored in -20$^{O}$C until use.

## Bacterial strains

Six MDR *A. baumannii* clinical isolates (3B, 30B, 38B, 78B, 98B, and 101B), all exhibiting carbapenem resistance, were selected from a collection previously published (Ventura et al. 2020), based on their genotypic profiles, antimicrobial susceptibility patterns and MIC values for carbapenems and phendione-based complexes. The MIC values ranged from 16 to 64 µg/mL for MEM (MG-MIC = 45.33 µg/mL); from 32 to 128 µg/mL for IMP (MG-MIC = 74.67 µg/mL); and from 0.78 to 1.56 µg/mL for both phendione-based complexes (MG-MIC = 1.43 µg/mL). Additionally, the carbapenem-susceptible reference strain *A. baumannii* ATCC 19606 was included. These information were summarized in Table S1 (Supplementary Information).

## Exposure-response curves

The antimicrobial activity and PD profiles of Ag-phendione and Cu-phendione were assessed using time-kill assay, conducted at different compound concentrations to create exposure-response curves, following the procedure outlined by Zhou et al. (2012), with minor adjustments. In brief, phendione-based complexes were diluted in cation-adjusted Mueller-Hinton broth (CAMHB) to final concentrations of 0.25×, 1×, 4× and 16× MIC value and inoculated with bacterial cultures in the logarithmic phase (~ 1 × $10^6$ CFU/mL). Cultures were incubated at 35 ± 2 ºC, and aliquots were collected at 0, 3, 6, 9, 12 and 24 h

for viable counts. For this, bacterial samples were serially diluted in 0.85% NaCl solution and plated on Mueller-Hinton agar (MHA) using the drop plate method (Miles et al. 1938). After 18–20 h of incubation at 35 ± 2 ºC, colonies were counted, and data were analyzed by plotting the $\log_{10}$ colony-forming unit per milliliter (CFU/mL) versus time (hours). The lower detection limit was established at $10^2$ CFU/mL. Bacteriostatic and bactericidal activities were defined as < 3 $\log_{10}$ and ≥ 3 $\log_{10}$ reductions in CFU/mL, respectively, relative to the starting inoculum (NCCLS 1999).

## Effects of dose fractionation

A short-term dose fractionation regimen was simulated for Ag-phendione and Cu-phendione to elucidate the kinetics of antimicrobial activity at sub-MIC concentrations under repeated exposure. Two doses, each corresponding to 0.5× MIC, were administered at a 6-hour interval according to the protocol described by Silva et al. (2011), with minor modifications. Test cultures were prepared by diluting the compounds in CAMHB and inoculating logarithmic-phase bacterial suspensions (~ 1 × $10^6$ CFU/mL). After 6 hours, a second dose was added. Positive controls included an untreated growth control and a single-dose treatment with 1× MIC. Cultures were incubated at 35 ± 2°C for 24 hours, and samples were collected at predetermined time points (0, 3, 6, 9, 12, and 24 hours) for viable cell quantification using the drop plate method (Miles et al. 1938). The results were graphically represented with $\log_{10}$ values of CFU/mL versus time, with a lower detection limit of $10^2$ CFU/mL.

## Post-antibiotic effect

PAE assays were conducted to determine the duration of bacterial growth suppression and regrowth kinetics following short-term exposure to Ag-phendione and Cu-phendione, as described by D'Atanasio et al. (2020), with minor modifications. Log-phase bacterial cultures in CAMHB were standardized to approximately 1 × $10^7$ CFU/mL and exposed to 1×, 5×, and 10× MIC concentrations of Ag-phendione or Cu-phendione for 1 hour at 35 ± 2°C. After exposure, the compounds were removed by a 1:1000 dilution in fresh, compound-free CAMHB, and cultures were subsequently re-incubated under the same conditions. A growth control, diluted without prior exposure to the phendione-based complexes, was included in each experiment. Viable counts were determined using the drop plate method (Miles et al. 1938) at the beginning of the experiment (t = − 1 h), immediately before and after compound removal by dilution (t = 0 h; two sampling points), and hourly for 5 hours thereafter. Results were expressed as $\log_{10}$ CFU/mL over time, with a lower limit of detection of $10^2$ CFU/mL. The PAE was calculated as the difference between the time required for the treated culture to increase by 1 $\log_{10}$ CFU/mL after drug removal (T) and the corresponding time for the untreated control (C), according to the formula PAE (h) = T − C, as previously described (Craig and Gudmundsson 1996). For comparative purposes, PAE curves were also generated for the reference antibiotics MEM and CIP using the same experimental protocol.

# Effect of bacterial density on MIC value

The influence of bacterial inoculum size on the MIC values of the phendione-based complexes was evaluated according to the methodology described by Jangra et al. (2019). Ag-phendione and Cu-phendione were serially diluted in CAMHB to final concentrations ranging from 0.78 to 50 µg/mL. MIC determinations were performed using five different inoculum densities ($10^4$, $10^5$, $10^6$, $10^7$, and $10^8$ CFU/mL). These inocula were prepared from bacterial suspensions in 0.85% NaCl adjusted to an optical density at 600 nm ($OD_{600}$) of 0.25 (approximately $10^9$ CFU/mL), followed by serial dilutions. Plates were incubated at 35 ± 2°C for 20–24 hours. After incubation, resazurin solution was added to each well, and the plates were further incubated for 1 hour to assess bacterial metabolic activity. MIC values were defined as the lowest compound concentration that prevented a color change, indicating inhibition of growth. The inoculum density was confirmed by viable cell counting using the drop plate method (Miles et al. 1938).

## Checkerboard

The interactions between phendione-based complexes and the carbapenems MEM and IMP against *A. baumannii* were evaluated using the checkerboard microdilution method, as described by Peregrino et al. (2021). The combinations tested were Ag-phendione + MEM, Cu-phendione + MEM, Ag-phendione + IMP, and Cu-phendione + IMP. Briefly, six two-fold serial dilutions of each agent prepared in CAMHB were dispensed into 96-well microtiter plates in a checkerboard configuration, enabling all possible concentration combinations (Pillai et al. 2005). Wells were inoculated with a bacterial suspension prepared in 0.85% NaCl to achieve a final inoculum of approximately $5 \times 10^5$ CFU/mL. Plates were incubated at 35 ± 2°C for 24 hours, and bacterial growth was assessed visually. Drug interactions were interpreted by calculating the fractional inhibitory concentration (FIC) for each agent in combination, followed by determination of the fractional inhibitory concentration index (FICI), defined as the sum of the individual FIC values. Interactions were classified as synergistic ($FICI \leq 0.5$), additive ($0.5 < FICI < 2$), indifferent ($2 \leq FICI < 4$), or antagonistic ($FICI > 4$). All experiments were performed with three independent biological replicates.

## Combination time-kill assay

The antimicrobial effects of phendione-based complexes in combination with MEM were assessed using time-kill assay, following the protocol described by Peregrino et al. (2021). In brief, CAMHB containing 0.5× MIC of each test compound, individually and in combination, was inoculated with log-phase bacterial cultures (~ $10^6$ CFU/mL). Cultures were incubated at 35 ± 2 ºC for 24 h, and samples were collected at 0, 3, 6, 9, 12 and 24 h for viable counts using the drop plate method (Miles et al. 1938). The data was represented graphically with $\log_{10}$ CFU/mL values plotted against time, with the lower limit of detection at $10^2$ CFU/mL. The results were interpreted in accordance with established guidelines (NCCLS 1999). Synergistic effects were defined as a $\geq 2$ $\log_{10}$ CFU/mL reduction in bacterial growth for the combination compared to the most active single agent at 24 h. Antagonism was defined by a $\geq 2$

$\log_{10}$ CFU/mL increase in growth after 24 h between the combination and the most active single agent. Indifference was defined as a < 2 $\log_{10}$ CFU/mL change at 24 h by the combination compared to the most active single agent.

# Potential to recalcitrance

The potential of phendione-based complexes to induce tolerance and heteroresistance was assessed using the Tolerance Disk Test (TDtest) described by Gefen et al. (2017), with minor adaptations. Sterile 6-mm filter paper discs were impregnated with 5 µL of Ag-phendione or Cu-phendione solution at 1000 µg/mL, a concentration selected based on preliminary optimization of inhibition zone diameters. After air-drying, the discs were placed onto MHA plates previously inoculated with bacterial suspensions (~ $1.5 \times 10^8$ CFU/mL) using a sterile swab. Plates were incubated at 35 ± 2°C for 24 hours, and the resulting inhibition zones were measured. Subsequently, the compound-containing discs were removed and replaced with new discs impregnated with 5 µL of sterile 40% glucose solution. Plates were re-incubated for an additional 24 hours under the same conditions and examined for regrowth within the original inhibition zones. The diameters of the inhibition halos after both incubation periods were measured and compared. Finally, subpopulations recovered from the inhibition zones were subjected to MIC determination by broth microdilution, following the methodology of Viganor et al. (2016).

# Statistics

All experiments were performed in triplicate, in three independent experimental sets. Data were expressed as mean ± standard deviation. The results were evaluated by Student's t-test or one-way ANOVA using Graphpad Prism 5. In all analyses, p-values ≤ 0.05 were considered statistically significant.

## Results and Discussion

# Exposure-response curves

The antimicrobial activity profiles of Ag-phendione and Cu-phendione were evaluated through exposure-response curves, revealing the relationship between compound antimicrobial activity, concentration and time of action. Both complexes exhibited effective antimicrobial effects, consistently reducing bacterial growth at concentrations equal to or above the MIC value. Ag-phendione exhibited consistent bactericidal activity against all seven *A. baumannii* isolates tested, as evidenced by inoculum reductions ≥ 3 $\log_{10}$ at 16× MIC value, particularly from 6 hours onward (Fig. 1). In contrast, Cu-phendione displayed variable, strain-dependent antibacterial activity, ranging from bacteriostatic to bactericidal effects. At 16× MIC, a ≥ 3 $\log_{10}$ reduction in viable cells was observed for two isolates (30B and 101B), while two others (78B and 98B) showed reductions greater than 2.4 $\log_{10}$ CFU/mL. The remaining three isolates exhibited only modest decreases in bacterial counts, approximately 1 $\log_{10}$ CFU/mL. Cu-phendione reached peak efficacy between 9 and 12 h (Fig. 2). These results are partially aligned with those reported by Galdino et al. (2019), who evaluated the time–kill kinetics of the same metal–phendione complexes

against *P. aeruginosa*. In that study, both Cu-phendione and Ag-phendione exhibited bactericidal activity at concentrations as low as 1× and 2× MIC, reinforcing the broad-spectrum antimicrobial potential of these metal-based compounds against distinct Gram-negative pathogens. The more pronounced bactericidal effect observed for Ag-phendione in the tested *A. baumannii* isolates may be attributed to the intrinsic antimicrobial properties of silver, which is widely recognized for its multifaceted modes of action, including disruption of bacterial membranes, generation of reactive oxygen species, and interaction with intracellular components (Frei et al. 2023).

Although both metal–phendione complexes consistently exhibited antimicrobial activity across the tested concentration range, the bacterial killing rates did not increase proportionally with higher compound concentrations, particularly during the early hours of exposure. This lack of a linear concentration-response relationship suggests that the antimicrobial activity of Ag-phendione and Cu-phendione is not strictly dose-dependent in the initial phases of treatment. Instead, these findings indicate a more prominent role for time-dependent dynamics in mediating their bactericidal effects. Such behavior is characteristic of time-dependent antimicrobial agents, for which sustained exposure above the MIC is more critical to efficacy than achieving high peak concentrations. Therefore, optimizing dosing regimens for these compounds may require strategies that prioritize prolonged drug exposure rather than escalation of dosage, aligning with PD principles observed in antibiotics such as β-lactams.

# Effects of dose fractionation

To investigate the influence of dose fractionation on antimicrobial activity, a two-dose regimen of the phendione-based metal complexes was evaluated (0.5× MIC administered at 0 and 6 hours). This fractionated dosing strategy resulted in significantly greater antimicrobial efficacy compared with a single administration at 1× MIC, highlighting the impact of exposure scheduling on antibacterial performance. Both complexes exhibited bactericidal effects between 3 and 6 hours after the second administration, resulting in complete eradication of *A. baumannii* in 86% (12/14) of the isolates tested (Figs. 3 and 4). These results reinforce the time-dependent PD profile previously described for these compounds, indicating that sustained exposure plays a pivotal role in maximizing bactericidal activity. The superior performance observed with fractionated dosing suggests that maintaining effective drug concentrations over time may be more critical than achieving high peak levels. To our knowledge, this is the first report examining dose fractionation for Ag-phendione and Cu-phendione against bacterial pathogens. Although further studies are needed to define therapeutic implications, these findings support that prolonged, lower-dose exposure strategies may enhance the antimicrobial potential of phendione-based complexes.

# Post-antibiotic effect

The PAE is a PD phenomenon characterized by the persistent suppression or delayed regrowth of bacteria following the removal of an antimicrobial agent (MacKenzie and Gould 1993; Zhanel et al. 1991; Gilberti et al. 2025). The PAE has a direct impact on dosing regimens and therapeutic strategies,

enabling extended dosing intervals and a broader therapeutic window (Gilberti et al. 2025). By reducing the number of required doses, a prolonged PAE may improve patient adherence, decrease the risk of adverse events and toxicity, and lower treatment costs (Zhanel et al. 1991; Drusano 2004; Quintiliani and Quintiliani 2008; Sun et al. 2022; Gilberti et al. 2025). Despite its therapeutic value, the molecular determinants of the PAE remain poorly understood (Gilberti et al. 2025). Proposed mechanisms include: (a) delayed bacterial regrowth due to reversible damage to critical cellular structures; (b) intracellular sequestration of antibiotics at specific binding sites or within the periplasmic space; (c) and prolonged persistence of the drug–target complex, which prevents immediate recovery of cellular function (MacKenzie and Gould 1993; Gilberti et al. 2025). Aminoglycosides, fluoroquinolones, macrolides and rifampin exhibit prolonged PAEs, which enable less frequent dosing without compromising therapeutic efficacy (Basak and Tonge 2020). By contrast, β-lactam antibiotics demonstrate minimal or no PAEs against Gram-negative bacteria, requiring frequent administration or continuous infusion to maintain effective drug concentrations (Basak and Tonge 2020).

In line with the aforementioned rationale, the PAE of Ag-phendione and Cu-phendione was investigated to determine their capacity to maintain antimicrobial activity after compound removal. PAE duration was calculated using the standard formula at a bactericidal concentration of 5× MIC value. Both complexes exhibited measurable PAE; however, Ag-phendione displayed a significantly longer average PAE duration compared to Cu-phendione: 1.857 ± 0.378 h versus 0.714 ± 0.488 h, respectively. This difference was further supported by distinct bacterial growth suppression patterns observed in the time–kill assays. As shown in the growth curves, bacterial cultures treated with Ag-phendione exhibited prolonged growth inhibition and a markedly delayed recovery phase (Fig. 5), whereas those exposed to Cu-phendione resumed growth more rapidly after compound withdrawal (Fig. 6). These divergent PAE profiles may reflect differences in the underlying mechanisms of action, despite the shared phendione ligand. The extended PAE associated with Ag-phendione suggests that it may induce more persistent cellular damage or prolonged metabolic impairment, highlighting its potential as a more effective agent for sustained antimicrobial activity. Although the antimicrobial activity of these complexes has been extensively described against a wide range of fungi (Granato et al. 2017, 2021; Rigo et al. 2023; Giovanini et al. 2025; de Mello et al. 2025), protozoa (Vargas-Rigo et al. 2019; Lima et al. 2021; Oliveira et al. 2023), and bacteria species (Viganor et al. 2016; Ventura et al. 2020; Peregrino et al. 2021; Rigo et al. 2023; Guerrieri et al. 2025), this study provides the first evidence characterizing the PAE of these compounds, thereby adding a novel PD dimension to their antimicrobial profile.

Additionally, PAE curves were generated for the reference antibiotics MEM and CIP to establish comparative benchmarks for the novel phendione-based metal complexes (Fig. S1 – Supplementary Information). The results revealed that the post-antibiotic recovery pattern of Cu-phendione closely mirrored that of MEM, which is known to elicit a relatively short PAE in Gram-negative bacteria (Pai et al. 2015). In contrast, the PAE profile of Ag-phendione aligned more closely with that of CIP, displaying extended recovery times that were markedly influenced by increasing compound concentrations (Pai et al. 2015). These parallels with well-characterized antibiotics provide valuable insights into the PD behavior of the phendione-based complexes, highlighting their potential for tailored dosing strategies.

Such information is critical for the design of future in vivo studies and may support the rational development of these compounds for clinical applications.

# Effect of CFU concentration on MIC

Considering that most antimicrobial susceptibility assays are performed under standardized bacterial density conditions (typically ~ 5 x $10^5$ CFU/mL), assessing the impact of variations in the initial inoculum concentration on MIC values is crucial (Loffredo et al. 2021). This information can later be incorporated into a PK/PD model, which, by considering the inoculum effect, proves to be more predictive in clinical scenarios (Rathi et al. 2016). The inoculum effect is generally described as a significant increase in the MIC when the inoculum size is increased (Brook 1989; Lenhard and Bulman 2019; Srivastava et al. 2026). Although no formal guideline definition exists, in literature, the in vitro inoculum effect is commonly defined as a ≥ 8-fold MIC increase using an inoculum 100-fold greater than the CLSI-recommended inoculum (Thomson and Moland 2001; Kang et al. 2004, 2014; Lopez-Cerero et al. 2010; Smith and Kirby 2018; Loffredo et al. 2021; Akrong et al. 2022; Chauzy et al. 2022). This effect is described for several species to classical antibiotics, such as β-lactams (Smith and Kirby 2018; Lenhard and Bulman 2019; Srivastava et al. 2026), but data regarding inoculum effect on *A. baumannii* is limited to a few studies. In a study with carbapenem-resistant *A. baumannii* isolates, IMP, colistin, rifampicin and tigecycline were not associated with this effect (Song et al. 2011). On the other hand, *A. baumannii* inoculum effect was described to polymyxin B using a strain isolated from a patient with meningitis (Akrong et al. 2022; Chauzy et al. 2022).

In this context, the influence of inoculum size on the MIC values of phendione-based complexes was evaluated (Tables 1 and 2). Comparing the standard inoculum concentration to the 100-fold higher ($10^7$ CFU/mL), it was observed a 2-fold increase in MIC values for all tested strains, except to 98B, in which Ag-phendione MIC remained the same. For most isolates, a $10^4$-fold increase in bacterial inoculum resulted in a 4-fold increase in MIC values, from 0.78 to 3.125 µg/mL. Despite this shift, the absolute increase in concentration was modest, with MIC values rising by up to 2.34 µg/mL in 92.9% of the tested strains. Notably, a concentration of 3.125 µg/mL (equivalent to 3.2 µM for Cu-phendione and 5 µM for Ag-phendione) was sufficient to inhibit the growth of 97.6% of all tested inocula. Only one clinical isolate (78B) exposed to Cu-phendione exhibited a more pronounced increase, reaching an 8-fold elevation in MIC at the highest inoculum tested. It is important to point out that these findings reflect a single-dose assessment and the inoculum effect might be attenuated under prolonged exposure, given the potentially time-dependent action of the compounds.

Table 1
Impact of varying inoculum sizes on the MIC values of Ag-phendione against six multidrug-resistant *Acinetobacter baumannii* clinical isolates and the ATCC 19606 strain.

| Code strains | Ag-phendione | | | | | |
|---|---|---|---|---|---|---|
| | $10^4$ | $10^5$ | $10^6$ | $10^7$ | $10^8$ | Final increase |
| ATCC 19606 | 0.78 | 0.78 | 1.56 | 1.56 | 3.12 | 4x |
| 3B | 0.78 | 0.78 | 0.78 | 1.56 | 3.12 | 4x |
| 30B | 0.78 | 0.78 | 0.78 | 1.56 | 3.12 | 4x |
| 38B | 0.78 | 0.78 | 0.78 | 1.56 | 3.12 | 4x |
| 78B | 0.78 | 0.78 | 0.78 | 1.56 | 1.56 | 2x |
| 98B | 0.78 | 0.78 | 0.78 | 0.78 | 1.56 | 2x |
| 101B | 0.39 | 0.39 | 0.39 | 0.78 | 1.56 | 4x |

Inoculum values are expressed in CFU/mL and MICs in µg/mL.

Table 2
Impact of varying inoculum sizes on the MIC values of Cu-phendione against six multidrug-resistant *Acinetobacter baumannii* clinical isolates and the ATCC 19606 strain.

| Code strains | Cu-phendione | | | | | |
|---|---|---|---|---|---|---|
| | $10^4$ | $10^5$ | $10^6$ | $10^7$ | $10^8$ | Final increase |
| ATCC 19606 | 0.78 | 1.56 | 1.56 | 3.12 | 3.12 | 4x |
| 3B | 0.78 | 0.78 | 0.78 | 1.56 | 3.12 | 4x |
| 30B | 0.78 | 0.78 | 0.78 | 1.56 | 3.12 | 4x |
| 38B | 0.78 | 0.78 | 0.78 | 1.56 | 3.12 | 4x |
| 78B | 0.78 | 0.78 | 0.78 | 1.56 | 6.25 | 8x |
| 98B | 0.78 | 0.78 | 0.78 | 1.56 | 3.12 | 4x |
| 101B | 0.39 | 0.39 | 0.39 | 0.78 | 1.56 | 4x |

Inoculum values are expressed in CFU/mL and MICs in µg/mL.

Overall, these findings suggest that the antimicrobial activity of both complexes remains preserved even under high inoculum conditions, with modest MIC shifts when the inoculum size is increased. Similarly, Jangra et al. (2019) reported consistent antimicrobial activity of the tridecaptin M peptide against a *K. pneumoniae* strain, with the MIC value remaining stable at 4 µg/mL across varying inoculum sizes

ranging from $10^5$ to $10^7$ CFU/mL and a two-fold increase in MIC value at $10^8$ CFU/mL concentration (Jangra et al. 2019). From a PD perspective, the limited magnitude of MIC escalation observed across increasing inocula supports the robustness of phendione-based complexes and suggests that clinically relevant bacterial loads are unlikely to compromise their antimicrobial activity.

# Checkerboard

The checkerboard assay was employed to evaluate the combinatorial efficacy of phendione-based complexes with carbapenem antibiotics across a broad range of concentrations. This approach enabled a comprehensive assessment of potential synergistic, additive, indifferent, or antagonistic interactions between the compounds. By systematically varying the concentrations of each agent, the method provided detailed insights into the PD relationships that may inform optimized combination therapy strategies against MDR *A. baumannii* isolates. The MIC and FICI values are presented in Tables 3 and 4, representing MEM and IMP combinations, respectively. The criteria used to determine the most effective concentration combinations were: (1) the demonstration of a synergistic interaction between the compounds; and (2) a reduction in the MIC values of the carbapenems, when combined with the test complexes, to levels below the clinical resistance breakpoints established by CLSI (2024).

Table 3
Checkerboard synergy analysis of meropenem combined with phendione-based complexes against six clinical *Acinetobacter baumannii* isolates and the ATCC 19606 strain.

| **Code strains** | **MIC of single agents (µg/mL)** | | | **MIC of the combination (FICI value)** | |
|---|---|---|---|---|---|
| | **MEM** | **Ag-phendione** | **Cu-phendione** | **MEM/Ag-phendione** | **MEM/Cu-phendione** |
| 3B | 32 | 0.78 | 1.56 | 16/0.39 (1.0)[b] | 16/0.78 (1.0)[b] |
| 30B | 32 | 1.56 | 1.56 | 16/0.39 (0.75)[b] | 8/0.78 (0.75)[b] |
| 38B | 16 | 1.56 | 1.56 | 8/0.39 (0.75)[b] | 4/0.78 (0.75)[b] |
| 78B | 16 | 1.56 | 1.56 | 4/0.78 (0.75)[b] | 8/0.39 (0.75)[b] |
| 98B | 64 | 0.78 | 1.56 | 16/0.39 (0.75)[b] | 16/0.78 (0.75)[b] |
| 101B | 64 | 1.56 | 1.56 | 16/0.78 (0.75)[b] | 16/0.78 (0.75)[b] |
| ATCC 19606 | 1 | 1.56 | 1.56 | 0.5/0.78 (1.0)[b] | 0.25/0.78 (0.75)[b] |

MEM – meropenem; [a] – synergy; [b] – additivity

Table 4
Checkerboard synergy analysis of imipenem combined with phendione-based complexes against six clinical *Acinetobacter baumannii* isolates and the ATCC 19606 strain.

| Code strains | MIC of single agents (µg/mL) | | | MIC of the combination (FICI value) | |
|---|---|---|---|---|---|
| | IMP | Ag-phendione | Cu-phendione | IMP/Ag-phendione | IMP/Cu-phendione |
| 3B | 64 | 1.56 | 1.56 | 32/0.39 (0.75)[b] | 32/0.78 (1.0)[b] |
| 30B | 32 | 1.56 | 1.56 | 8/0.78 (0.75)[b] | 8/0.39 (0.5)[a] |
| 38B | 16 | 1.56 | 1.56 | 4/0.39 (0.5)[a] | 4/0.39 (0.5)[a] |
| 78B | 16 | 1.56 | 1.56 | 4/0.39 (0.5)[a] | 8/0.78 (1.0)[b] |
| 98B | 32 | 0.78 | 1.56 | 8/0.39 (0.75)[b] | 8/0.39 (0.75)[b] |
| 101B | 64 | 0.78 | 1.56 | 32/0.19 (0.75)[b] | 16/0.78 (0.75)[b] |
| ATCC 19606 | 1 | 1.56 | 1.56 | 0.5/0.78 (1.0)[b] | 0.5/0.78 (1.0)[b] |

IMP – imipenem; [a] – synergy; [b] – additivity

FICI values for the combinations of both Ag-phendione and Cu-phendione with IMP ranged from 0.5 to 1.0, consistently indicating either synergistic or additive interactions across all tested *A. baumannii* isolates. In contrast, combinations involving MEM resulted exclusively in additive effects. Notably, synergistic interactions were observed in 28.57% and 14.29% of the isolates when IMP was combined with Ag-phendione and Cu-phendione, respectively. Similarly, Peregrino et al. (2021) demonstrated the in vitro efficacy of Ag-phendione and Cu-phendione in combination with carbapenems against KPC-producing *K. pneumoniae* clinical strains. Using the checkerboard assay, the authors primarily observed additive interactions for IMP combinations, whereas MEM combinations exhibited a high frequency of synergistic effects. Furthermore, no indifferent or antagonistic activities were found for any of the combinations used on the tested isolates (Peregrino et al. 2021). This study results are consistent with those findings, as neither investigation reported indifferent or antagonistic interactions. Together, these data reinforce the therapeutic potential of combining carbapenems with phendione-based metal complexes, which can be an alternative strategy for the treatment of infections caused by MDR Gram-negative pathogens. Additional evidence supporting the combinatorial potential of phendione-based metal complexes has been reported in other microorganisms. Vargas-Rigo et al. (2019) observed a synergistic interaction between Cu-phendione and metronidazole (MTZ) against MTZ-resistant *Trichomonas vaginalis* isolates. Similarly, in ampicillin (AMP) and tetracycline (TET) resistant enteroaggregative *Escherichia coli* (EAEC) isolates, most combinations of AMP or TET with either Cu-phendione or Ag-phendione resulted in additive effects. Synergistic interactions were also documented for TET + Cu-phendione, AMP + Ag-phendione, and TET + Ag-phendione (Guerrieri et al. 2025).

To further validate the predominance of additive interactions, five additional strains from the original collection of 26 *A. baumannii* clinical isolates were included in the checkerboard assay (Tables S2 and S3 – Supplementary Information). Consistent with previous results, all tested combinations in the additional strains demonstrated exclusively additive effects. Remarkably, these additive interactions were accompanied by significant reductions in the MIC values of MEM, underscoring their pharmacological relevance. In the MEM + Ag-phendione combination, MEM MICs were reduced 4-fold in 45.45% (5/11) and 8-fold in 18.18% (2/11) of the clinical isolates. Similarly, the MEM + Cu-phendione combination led to a 4-fold MIC reduction in 36.36% (4/11) of the strains. Importantly, these reductions lowered the MEM MIC values below the CLSI (2024) resistance breakpoint in 27.27% (3/11) of the isolates, reclassifying them within the intermediate susceptibility category. These findings further support the clinical relevance of combining MEM, or potentially other antibiotics, with phendione-based metal complexes.

# Combination time-kill assay

Time-kill assays were performed to validate the antimicrobial activity of Ag-phendione and Cu-phendione in combination with MEM. This method is considered the gold standard for synergism evaluation of drug combinations (Sopirala et al. 2010; Gaudereto et al. 2020), as it provides dynamic, time-dependent information on bacterial killing kinetics, offering insights that cannot be obtained by endpoint-based methods (Gaudereto et al. 2020). Consistent with the checkerboard assay findings, no significant synergistic effects were detected in any of the tested combinations (Figs. 8 and 9). Nonetheless, a notable reduction in bacterial growth was observed in the combination treatment curves when compared to the untreated growth controls. Interestingly, the time-kill profiles of the combinations closely resembled those of the phendione-based complexes alone, suggesting that the observed effects were primarily driven by the intrinsic activity of the complexes rather than by a potentiated interaction with MEM. In contrast, Peregrino et al. (2021) found synergistic effects for combinations of MEM and phendione-based complexes against *K. pneumoniae*. This discrepancy may be due to the differences in MIC values between the two species. The geometric mean MIC of Cu-phendione and Ag-phendione against *K. pneumoniae* is 9.88 and 10.1 μM, respectively, whereas against *A. baumannii*, the values are 1.63 and 2.48 μM. Consequently, concentrations of 0.5× MIC for *A. baumannii* are expected to be more effective due to their closer proximity to the MIC value. Additionally, consistent with the findings of Peregrino et al. (2021) on *K. pneumoniae*, Cu-phendione and Ag-phendione demonstrate their maximum efficacy around 9 h after application. Furthermore, the significant differences in bacterial loads between cultures treated with the combinations and those exposed to MEM alone, along with the absence of any antagonistic effects, support the ability of these compounds to enhance MEM's antimicrobial activity. This becomes particularly relevant in cases of carbapenem resistance, where the need for alternative and effective treatment strategies is critical.

# Potential to recalcitrance

To assess the potential induction of tolerance and heteroresistance by Ag-phendione and Cu-phendione, a modified version of the TDtest, as described by Gefen et al. (2017), was used. Initial tests showed

inhibition zone diameters ranging from 16 to 21 mm for both metal complexes. Following the second incubation, during which the original compound-containing disc was replaced with a glucose-impregnated disc, only minimal reductions (≤ 1 mm) or no change in inhibition zone diameters were observed, suggesting the absence of tolerant or heteroresistant subpopulations. To further validate these findings and increase the likelihood of detecting antimicrobial recalcitrance, the assay was extended to additional 20 *A. baumannii* clinical isolates previously characterized by Ventura et al. (2020). The results from the additional strains were consistent with the initial observations, with inhibition zones ranging from 16 to 23 mm and negligible or no reduction in halo diameter after the second incubation. These findings suggest a low propensity of Ag-phendione and Cu-phendione to induce tolerance or heteroresistance under the tested conditions.

Regarding colony growth within the inhibition zone, no consistent pattern indicative of tolerance, as characterized by Gefen et al. (2017), was observed. However, isolated colonies frequently appeared near the edge of confluent bacterial growth after the initial 24-h incubation. This pattern was noted in at least one biological replicate for 23 isolates treated with Cu-phendione and 15 isolates treated with Ag-phendione. Following removal of the compound-containing disc and replacement with a glucose-impregnated disc, no increase in colony number was detected during the subsequent 24 h; however, an increase in colony size was observed. According to the original TDtest criteria, the emergence of colonies within the inhibition zone during the first 24h may suggest heteroresistance. Nonetheless, this interpretation does not appear to be applicable to the compounds under investigation. MIC determinations for subpopulations isolated from these regions revealed values identical or closely similar to those of the parental strains (Table 5), indicating an absence of heteroresistant variants. Given the lack of prior studies on the diffusion behavior of phendione-based complexes in solid agar media, it is plausible that the irregular growth patterns observed could be attributed to heterogeneous diffusion dynamics rather than to antimicrobial recalcitrance. Further investigation into the physicochemical diffusion properties of these compounds is warranted to better understand this phenomenon. Moreover, the inclusion of a comparator antibiotic with a well-established tendency to display heteroresistance under identical experimental conditions would provide a useful internal reference and strengthen the interpretation of these findings. Therefore, further studies are warranted to evaluate the complexes long-term resistance induction potential.

Table 5
Results of the modified disk diffusion assay for 26 clinical isolates of *Acinetobacter baumannii* and the ATCC 19606 strain.

| | MIC of Cu-phendione (µg/mL) | | | MIC of Ag-phendione (µg/mL) | | |
|---|---|---|---|---|---|---|
| | **MIC Parental** | **MIC Derivative[1]** | **MIC Derivative[2]** | **MIC Parental** | **MIC Derivative[1]** | **MIC Derivative[2]** |
| **ATCC 19606** | 1.56 | ND | 3.12 | 1.56 | ND | 3.12 |
| **3B** | 1.56 | ND | 6.25 | 1.56 | ND | ND |
| **8B** | 1.56 | ND | ND | 1.56 | 1.56 | ND |
| **22B** | 1.56 | 6.25 | 6.25 | 1.56 | 3.12 | 3.12 |
| **24B** | 1.56 | 1.56 | ND | 1.56 | 0.78 | ND |
| **25B** | 1.56 | 1.56 | ND | 1.56 | 1.56 | ND |
| **30B** | 1.56 | 3.12 | 3.12 | 1.56 | 3.12 | 3.12 |
| **37B** | 1.56 | 3.12 | 6.25 | 1.56 | 1.56 | 3.12 |
| **38B** | 1.56 | 6.25 | 3.12 | 1.56 | ND | 3.12 |
| **57B** | 1.56 | 3.12 | 3.12 | 1.56 | 1.56 | ND |
| **71B** | 1.56 | 3.12 | 6.25 | 1.56 | 1.56 | 3.12 |
| **76B** | 1.56 | 3.12 | ND | 1.56 | 1.56 | ND |
| **78B** | 1.56 | ND | 3.12 | 1.56 | ND | 1.56 |
| **80B** | 1.56 | 3.12 | 6.25 | 1.56 | 1.56 | 3.12 |
| **92B** | 1.56 | ND | 1.56 | 1.56 | ND | ND |
| **96B** | 6.25 | ND | ND | 1.56 | ND | ND |
| **97B** | 1.56 | ND | ND | 1.56 | ND | ND |
| **98B** | 1.56 | ND | 3.12 | 1.56 | ND | ND |
| **99B** | 1.56 | 3.12 | 6.25 | 1.56 | ND | ND |
| **101B** | 1.56 | ND | 3.12 | 1.56 | ND | ND |
| **102B** | 1.56 | ND | 1.56 | 1.56 | ND | 1.56 |
| **106B** | 1.56 | 3.12 | 3.12 | 1.56 | 3.12 | 1.56 |
| **108B** | 1.56 | 3.12 | 3.12 | 1.56 | ND | ND |
| **109B** | 1.56 | ND | 6.25 | 1.56 | ND | ND |

| | MIC of Cu-phendione (µg/mL) | | | MIC of Ag-phendione (µg/mL) | | |
|---|---|---|---|---|---|---|
| | **MIC Parental** | **MIC Derivative[1]** | **MIC Derivative[2]** | **MIC Parental** | **MIC Derivative[1]** | **MIC Derivative[2]** |
| **111B** | 1.56 | 3.12 | 3.12 | 1.56 | ND | ND |
| **117B** | 1.56 | 3.12 | 3.12 | 1.56 | 3.12 | 1.56 |
| **125B** | 1.56 | 3.12 | ND | 1.56 | 3.12 | ND |

[1] MIC values of the 1st independent experiment; [2] MIC values of the 2nd independent experiment; ATCC – reference strain ATCC 19606; ND – not determined, indicates tests in which no colonies were isolated within the growth inhibition zone.

Taken together, our results highlight the potent antimicrobial activity and favorable PD profiles of both metal-based complexes against MDR *A. baumannii* strains, with Ag-phendione demonstrating exclusively bactericidal effects, whereas Cu-phendione exhibited a mixed profile of bactericidal and bacteriostatic activity. Both complexes achieved peak efficacy between 6 and 12 h post-exposure and displayed predominantly time-dependent killing kinetics. Importantly, Ag-phendione exhibited a significantly prolonged PAE, and both complexes showed minimal inoculum effect and no incipient evidence of recalcitrance or resistance induction. Furthermore, the consistent efficacy of Ag-phendione and Cu-phendione under varied experimental conditions (whether used alone or in combination with conventional antibiotics) reinforces their potential therapeutic application, particularly in the context of difficult-to-treat, drug-resistant infections. These results are further supported by previous studies reporting broad-spectrum antimicrobial activity, as well as good safety and tolerability profiles. Collectively, these findings highlight phendione-based complexes as potential alternatives to current antimicrobial regimens, offering new strategies to overcome resistance mechanisms prevalent in high-priority bacterial pathogens. Future investigations should prioritize the characterization of the pharmacokinetic (PK) properties of these compounds to enable integrated PK/PD modeling and simulation studies. Advancing our understanding of phendione-based complexes may ultimately contribute to the development of innovative treatment options in the ongoing fight against antimicrobial resistance.

## Declarations

# Conflicts of Interest:

The authors declare that there are no conflicts of interest.

# Funding:

This work was financially supported by Fundação de Amparo à Pesquisa e Inovação do Espírito Santo (FAPES); Fundação Carlos Chagas Filho de Amparo à Pesquisa do Estado do Rio de Janeiro (FAPERJ); Conselho Nacional de Desenvolvimento Científico e Tecnológico (CNPq); and Coordenação de Aperfeiçoamento de Pessoal de Nível Superior (CAPES). Lívia de Souza Ramos was supported by FAPERJ E-26/203.103/2026.

# Author Contribution

Conceptualization: Ingrid Vianez Peregrino, Luiz Felipe Vieira dos Santos Amorim, Roberta Ferreira Ventura Mendes, Ana Paula Ferreira Nunes, André Luis Souza dos Santos. Methodology and investigation: Ingrid Vianez Peregrino, Luiz Felipe Vieira dos Santos Amorim, Roberta Ferreira Ventura Mendes. Formal analysis and data curation: Ingrid Vianez Peregrino, Gabriela Seabra, Luiz Felipe Vieira dos Santos Amorim, Roberta Ferreira Ventura Mendes, Ana Paula Ferreira Nunes, Livia de Souza Ramos, André Luis Souza dos Santos. Resources: Ana Paula Ferreira Nunes, André Luis Souza dos Santos, Michael Devereux, Malachy McCann. Supervision: Ana Paula Ferreira Nunes, André Luis Souza dos Santos. Writing (original draft): Ingrid Vianez Peregrino, Gabriela Seabra. Writing (review and editing): Gabriela Seabra, Ana Paula Ferreira Nunes, Lívia de Souza Ramos, André Luis Souza dos Santos. All authors read and approved the final manuscript.

# Acknowledgement

The authors extend their gratitude to all collaborators at the RESBAC Laboratory (Federal University of Espírito Santo), particularly Caio Ferrighetto, for his support in conducting the research.

## References

1. Akrong G, Chauzy A, Aranzana-Climent V, Lacroix M, Deroche L, Prouvensier L et al (2022) A new pharmacokinetic-pharmacodynamic model to characterize the inoculum effect of *Acinetobacter baumannii* on polymyxin B *in vitro*. Antimicrob Agents Chemother 66:e0178921. https://doi.org/10.1128/AAC.01789-21
2. Baran A, Kwiatkowska A, Potocki L (2023) Antibiotics and bacterial resistance – A short story of an endless arms race. Int J Mol Sci 24:5777. https://doi.org/10.3390/ijms24065777
3. Basak S, Tonge PJ (2020) Drug target residence time and the pharmacodynamics of antibacterial agents, In: Bronson JJ, Med Chem Rev, Vol. 55, Washington, DC: Medicinal Chemistry Division of the American Chemical Society, 367–380
4. Bissantz C, Zampaloni C, David-Pierson P, Dieppois G, Guenther A, Trauner A et al (2024) Translational PK/PD for the development of novel antibiotics – A drug developer's perspective. Antibiotics 13:72. https://doi.org/10.3390/antibiotics13010072
5. Brook I (1989) Inoculum effect. Rev Infect Dis 1:361–368. https://doi.org/10.1093/clinids/11.3.361

6. Cavallo I, Oliva A, Pages R, Sivori F, Truglio M, Fabrizio G et al (2023) *Acinetobacter baumannii* in the critically ill: Complex infections get complicated. Front Microbiol 14:1–17. https://doi.org/10.3389/fmicb.2023.1196774
7. Chauzy A, Akrong G, Aranzana-Climent V, Moreau J, Prouvensier L, Mirfendereski H et al (2022) PKPD modeling of the inoculum effect of *Acinetobacter baumannii* on polymyxin B in vivo. Front Pharmacol 3:842921. https://doi.org/10.3389/fphar.2022.842921
8. Claudel M, Schwarte JV, Fromm KM (2020) New antimicrobial strategies based on metal complexes. Chemistry 2:849–899. https://doi.org/10.3390/chemistry2040056
9. CLSI (2024) Clinical and Laboratory Standards Institute. M100-Ed34: Performance standards for antimicrobial susceptibility testing, 34th Edition; Wayne, PA, USA
10. Craig WA, Gudmundsson S (1996) Postantibiotic effect. In: Lorian V (ed) Antibiotics in laboratory medicine, 4 edn. Williams & Wilkins, Baltimore, pp 296–329
11. D'Atanasio N, De Joannon AC, Di Sante L, Mangano G, Ombrato R, Vitiello M et al (2020) Antibacterial activity of novel dual bacterial DNA type II topoisomerase inhibitors. PLoS ONE 15:e0228509. https://doi.org/10.1371/journal.pone.0228509
12. de Mello TP, da Silva BA, Lione V, Devereux M, McCann M, Branquinha MH et al (2025) Impact of copper(II) and silver(I) complexes containing 1,10-phenanthroline-5,6-dione on cellular and virulence aspects of *Scedosporium apiospermum*. Curr Top Med Chem 25:1377–1388. https://doi.org/10.2174/0115680266327984241018111547
13. Drusano GL (2004) Antimicrobial pharmacodynamics: Critical interactions of 'bug and drug'. Nat Rev Microbiol 2:289–300. https://doi.org/10.1038/nrmicro862
14. Evans A, Kavanagh KA (2021) Evaluation of metal-based antimicrobial compounds for the treatment of bacterial pathogens. J Med Microbiol 70:1–18. https://doi.org/10.1099/jmm.0.001363
15. Frei A, Verderosa AD, Elliott AG, Zuegg J, Blaskovich MAT (2023) Metals to combat antimicrobial resistance. Nat Rev Chem 7:202–224. https://doi.org/10.1038/s41570-023-00463-4
16. Frota HF, Barbosa PF, Lorentino CMA, Affonso LRF, Ramos LS, Oliveira SSC et al (2024) Unveiling the antifungal mechanisms of CTP, a new copper(II)-theophylline/1,10-phenanthroline complex, on drug-resistant non-albicans *Candida* species. Biometals 37:1237–1253. https://doi.org/10.1007/s10534-024-00605-1
17. Galdino ACM, Viganor L, de Castro AA, da Cunha EFF, Mello TP, Mattos LM et al (2019) Disarming *Pseudomonas aeruginosa* virulence by the inhibitory action of 1,10-phenanthroline-5,6-dione-based compounds: Elastase B (LasB) as a chemotherapeutic target. Front Microbiol 10:1701. https://doi.org/10.3389/fmicb.2019.01701
18. Galdino ACM, Viganor L, Pereira MM, Devereux M, McCann M, Branquinha MH et al (2022) Copper(II) and silver(I)-1,10-phenanthroline-5,6-dione complexes interact with double-stranded DNA: Further evidence of their apparent multi-modal activity towards *Pseudomonas aeruginosa*. J Biol Inorg Chem 27:201–213. https://doi.org/10.1007/s00775-021-01922-3

19. Gandra RM, Pacheco CA, Sangenito LS, Ramos LS, Souza LO, McCarron P et al (2024) Manganese(II), copper(II) and silver(I) complexes containing 1,10-phenanthroline/1,10-phenanthroline-5,6-dione against *Candida* species. Future Microbiol 19:385–395. https://doi.org/10.2217/fmb-2023-0212
20. Gaudereto JJ, Neto LVP, Leite GC, Espinoza EPS, Martins RCR, Villas Boa Prado G et al (2020) Comparison of methods for the detection of in vitro synergy in multidrug-resistant Gram-negative bacteria. BMC Microbiol 20:97. https://doi.org/10.1186/s12866-020-01756-0
21. GBD 2021 Antimicrobial Resistance Collaborators (2024) Global burden of bacterial antimicrobial resistance 1990–2021: A systematic analysis with forecasts to 2050. Lancet 404:1199–1226. https://doi.org/10.1016/S0140-6736(24)01867-1
22. Gefen O, Chekol B, Strahilevitz J, Balaban NQ (2017) TDtest: Easy detection of bacterial tolerance and persistence in clinical isolates by a modified disk-diffusion assay. Sci Rep 7:1–9. https://doi.org/10.1038/srep41284
23. Gilberti AL, Tu MM, Rachwalski K, Ali MI, Cohen SA, Akoglu M et al (2025) Identifying modulators of the post-antibiotic effect. ACS Infect Dis 11:2542–2552. https://doi.org/10.1021/acsinfecdis.5c00424
24. Giovanini L, Casemiro AL, Corrêa LS, Mendes M, Mello TP, Souza LOP et al (2025) Toxicity assessment and antifungal potential of copper(ii) and silver(i) complexes with 1,10-phenanthroline-5,6-dione against drug-resistant clinical isolates of *Cryptococcus gattii* and *Cryptococcus neoformans*. J Fungi (Basel) 11:436. https://doi.org/10.3390/jof11060436
25. Granato MQ, Gonçalves DS, Seabra SH, McCann M, Devereux M, Dos Santos AL et al (2017) 1,10-phenanthroline-5,6-dione-based compounds are effective in disturbing crucial physiological events of *Phialophora verrucosa*. Front Microbiol 8:76. https://doi.org/10.3389/fmicb.2017.00076
26. Granato MQ, Mello TP, Nascimento RS, Pereira MD, Rosa TLSA, Pessolani MCV et al (2021) Silver(I) and copper(II) complexes of 1,10-phenanthroline-5,6-dione against *Phialophora verrucosa*: A focus on the interaction with human macrophages and *Galleria mellonella* larvae. Front Microbiol 12:641258. https://doi.org/10.3389/fmicb.2021.641258
27. Guerrieri CG, Sagrillo MVM, Vinhas SA, Devereux M, McCann M, de Mello TP et al (2025) Combating enteroaggregative *Escherichia coli*: Dual antibacterial and antibiofilm effects of silver- and copper-1,10-phenanthroline-5,6-dione complexes. AIMS Microbiol 11:855–876. https://doi.org/10.3934/microbiol.2025036
28. Gupta R, Sharma S (2022) Role of alternatives to antibiotics in mitigating the antimicrobial resistance crisis. Indian J Med Res 156:464. https://doi.org/10.4103/ijmr.ijmr_3514_20
29. Jangra M, Kaur M, Podia M, Tambat R, Singh V, Chandal N et al (2019) Purification and biological activity of natural variants synthesized by tridecaptin M gene cluster and in vitro drug-kinetics of this antibiotic class. Sci Rep 9:1–10. https://doi.org/10.1038/s41598-019-54716-8
30. Jorda A, Zeitlinger M (2020) Preclinical pharmacokinetic/pharmacodynamic studies and clinical trials in the drug development process of EMA-approved antibacterial agents: A review. Clin

Pharmacokinet 59:1071–1084. https://doi.org/10.1007/s40262-020-00892-0

31. Kang CI, Pai H, Kim SH, Kim HB, Kim EC, Oh MD et al (2004) Cefepime and the inoculum effect in tests with *Klebsiella pneumoniae* producing plasmid-mediated AmpC-type beta-lactamase. J Antimicrob Chemother 54:1130–1133. https://doi.org/10.1093/jac/dkh462
32. Kang CI, Cha MK, Kim SH, Wi YM, Chung DR, Peck KR et al (2014) Extended-spectrum cephalosporins and the inoculum effect in tests with CTX-M-type extended-spectrum β-lactamase-producing *Escherichia coli*: Potential clinical implications of the revised CLSI interpretive criteria. Int J Antimicrob Agents 43:456–459. https://doi.org/10.1016/j.ijantimicag.2014.01.030
33. Lenhard JR, Bulman ZP (2019) Inoculum effect of β-lactam antibiotics. J Antimicrob Chemother 74:2825–2843. https://doi.org/10.1093/jac/dkz226
34. Li Q, Zhou X, Yang R, Shen X, Li G, Zhang C et al (2024) Carbapenem-resistant Gram-negative bacteria (CR-GNB) in ICUs: Resistance genes, therapeutics, and prevention – A comprehensive review. Front Public Health 12:1–13. https://doi.org/10.3389/fpubh.2024.1376513
35. Lima AKC, Elias CGR, Oliveira SSC, Santos-Mallet JR, McCann M, Devereux M, Branquinha MH et al (2021) Anti-*Leishmania braziliensis* activity of 1,10-phenanthroline-5,6-dione and its Cu(II) and Ag(I) complexes. Parasitol Res 120:3273–3285. https://doi.org/10.1007/s00436-021-07265-x
36. Lister PD (2006) The role of pharmacodynamic research in the assessment and development of new antibacterial drugs. Biochem Pharmacol 71:1057–1065. https://doi.org/10.1016/j.bcp.2005.10.038
37. Loffredo MR, Savini F, Bobone S, Casciaro B, Franzyk H, Mangoni ML et al (2021) Inoculum effect of antimicrobial peptides. Proc Natl Acad Sci USA 118:e2014364118. https://doi.org/10.1073/pnas.2014364118
38. Lopez-Cerero L, Picon E, Morillo C, Hernandez JR, Docobo F, Pachon J et al (2010) Comparative assessment of inoculum effects on the antimicrobial activity of amoxycillin-clavulanate and piperacillin-tazobactam with extended-spectrum beta-lactamase-producing and extended-spectrum beta-lactamase-nonproducing *Escherichia coli* isolates. Clin Microbiol Infect 16:132–136. https://doi.org/10.1111/j.1469-0691.2009.02893.x
39. MacKenzie FM, Gould IM (1993) The post-antibiotic effect. J Antimicrob Chemother 32. https://doi.org/10.1093/jac/32.4.519. :519 – 37
40. MacNair CR, Rutherford ST, Tan M-W (2023) Alternative therapeutic strategies to treat antibiotic-resistant pathogens. Nat Rev Microbiol 22:262–275. https://doi.org/10.1038/s41579-023-00993-0
41. Mancuso G, De Gaetano S, Midiri A, Zummo S, Biondo C (2023) The challenge of overcoming antibiotic resistance in carbapenem-resistant Gram-negative bacteria: Attack on titan. Microorganisms. https://doi.org/10.3390/microorganisms11081912. 11:1912
42. McCann M, Coyle B, McKay S, McCormack P, Kavanagh K, Devereux M et al (2004) Synthesis and X-ray crystal structure of $[Ag(phendio)_2]ClO_4$ (phendio = 1,10-phenanthroline-5,6-dione) and its effects on fungal and mammalian cells. Biometals 17:635–645. https://doi.org/10.1007/s10534-004-1229-5

43. McCann M, Santos ALS, Da Silva BA, Romanos MTV, Pyrrho AS, Devereux M et al (2012) In vitro and in vivo studies into the biological activities of 1,10-phenanthroline, 1,10-phenanthroline-5,6-dione and its copper(ii) and silver(i) complexes. Toxicol Res 1:47–54. https://doi.org/10.1039/c2tx00010e
44. Miles AA, Misra SS, Irwin JO (1938) The estimation of the bactericidal power of the blood. Epidemiol Infect 38:732–749. https://doi.org/10.1017/s002217240001158x
45. Minichmayr IK, Aranzana-Climent V, Friberg LE (2022) Pharmacokinetic/pharmacodynamic models for time courses of antibiotic effects. Int J Antimicrob Agents 60:106616. https://doi.org/10.1016/j.ijantimicag.2022.106616
46. Mohan B, Choudhary M (2021) Synthesis, crystal structure, computational study and anti-virus effect of mixed ligand copper (II) complex with ONS donor Schiff base and 1, 10-phenanthroline. J Mol Struct 1246:131246. https://doi.org/10.1016/j.molstruc.2021.131246
47. Mozhayskiy V, Tagkopoulos I (2013) Microbial evolution in vivo and in silico: Methods and applications. Integr Biol 5:262–277. https://doi.org/10.1039/c2ib20095c
48. ; NCCLS. National Committee for Clinical Laboratory Standards. Methods for determining bactericidal activity of antimicrobial agents; Approved guideline, NCCLS document M26-A, Wayne (1999) PA, USA
49. O'Shaughnessy M, Piatek M, McCarron P, McCann M, Devereux M, Kavanagh K et al (2022) In vivo activity of metal complexes containing 1,10-phenanthroline and 3,6,9-trioxaundecanedioate ligands against *Pseudomonas aeruginosa* infection in *Galleria mellonella* larvae. Biomedicines 10:222. https://doi.org/10.3390/biomedicines10020222
50. Oliveira SSC, Santos VS, Devereux M, McCann M, Santos ALS, Branquinha MH (2023) The anti-*Leishmania amazonensis* and anti-*Leishmania chagasi* action of copper(II) and silver(I) 1,10-phenanthroline-5,6-dione coordination compounds. Pathogens 12:70. https://doi.org/10.3390/pathogens12010070
51. Pai M, Cottrell M, Kashuba A, Bertino J (2015) Pharmacokinetics and pharmacodynamics of anti-infective agents. In: Bennett J, Dolin R, Blaser M (eds) Mandell, Douglas, and Bennett's principles and practice of infectious diseases, 8 edn. Elsevier, Philadelphia, pp 252–262. https://doi.org/10.1016/B978-1-4557-4801-3.00019-9
52. Palmer ME, Andrews LJ, Abbey TC, Dahlquist AE, Wenzler E (2022) The importance of pharmacokinetics and pharmacodynamics in antimicrobial drug development and their influence on the success of agents developed to combat resistant gram-negative pathogens: A review. Front Pharmacol 13:1–10. https://doi.org/10.3389/fphar.2022.888079
53. Peregrino IV, Ventura RF, Borghi M, Schuenck RP, Devereux M, McCann M et al (2021) Antibacterial activity and carbapenem re-sensitizing ability of 1,10-phenanthroline-5,6-dione and its metal complexes against KPC-producing *Klebsiella pneumoniae* clinical strains. Lett Appl Microbiol 73:139–148. https://doi.org/10.1111/lam.13485
54. Pillai SK, Moellering RC, Eliopoulos GM (2005) Antimicrobial combinations. In: Lorian V (ed) Antibiotics in laboratory medicine, 5 edn. Lippincott Williams & Wilkins Co, Philadelphia, pp 365–440

55. Quintiliani R, Sr, Quintiliani R Jr (2008) Pharmacokinetics/pharmacodynamics for critical care clinicians. Crit Care Clin 24:335–48, xi. https://doi.org/10.1016/j.ccc.2007.12.008
56. Rakshit T, Haldar A, Jana S, Raha S, Saha R, Mandal D (2023) A brief review on the antimicrobial activity of transition metal complexes with N,O donor chelating ligand. Results Chem 6:101224. https://doi.org/10.1016/j.rechem.2023.101224
57. Rathi C, Lee RE, Meibohm B (2016) Translational PK/PD of anti-infective therapeutics. Drug Discov Today Technol 21–22:41–49. https://doi.org/10.1016/j.ddtec.2016.08.004
58. Rigo GV, Cardoso FG, Devereux M, McCann M, Macedo AJ, Santos ALS et al (2023) Antimicrobial and antibiofilm activities of copper(II)-1,10-phenanthroline-5,6-pione against commensal bacteria and fungi responsible for vaginal microbiota dysbiosis. Curr Microbiol 80:383. https://doi.org/10.1007/s00284-023-03500-z
59. Rodríguez-Gascón A, Solinís MÁ, Isla A (2021) The role of PK/PD analysis in the development and evaluation of antimicrobials. Pharmaceutics 13:833. https://doi.org/10.3390/pharmaceutics13060833
60. Santos ALS, Lima AKC, Oliveira SSC, Santos RFD, Devereux M, McCann M et al (2022) Decoding the anti-*Leishmania braziliensis* activity of 1,10-phenanthroline-5,6-dione and its silver- and copper-based complexes: In vitro and in vivo approaches. Eur J Med Chem Rep 6:100093. https://doi.org/10.1016/j.ejmcr.2022.100093
61. Silva LV, Araújo MT, Santos KRND, Nunes APF (2011) Evaluation of the synergistic potential of vancomycin combined with other antimicrobial agents against methicillin-resistant *Staphylococcus aureus* and coagulase-negative *Staphylococcus* spp strains. Mem Inst Oswaldo Cruz 106:44–50. https://doi.org/10.1590/s0074-02762011000100007
62. Smith KP, Kirby JE (2018) The inoculum effect in the era of multidrug resistance: Minor differences in inoculum have dramatic effect on MIC determination. Antimicrob Agents Chemother 62:e00433–e00418. https://doi.org/10.1128/AAC.00433-18
63. Song JY, Cheong HJ, Choi WS, Heo JY, Noh JY, Kim WJ (2011) Clinical and microbiological characterization of carbapenem-resistant *Acinetobacter baumannii* bloodstream infections. J Med Microbiol 60:605–611. https://doi.org/10.1099/jmm.0.029439-0
64. Sopirala MM, Mangino JE, Gebreyes WA, Biller B, Bannerman T, Balada-Llasat JM et al (2010) Synergy testing by Etest, microdilution checkerboard, and time-kill methods for pan-drug-resistant a *Acinetobacter baumannii*. Antimicrob Agents Chemother 54:4678–4683. https://doi.org/10.1128/AAC.00497-10
65. Sousa IS, Vieira TDP, Menna-Barreto RFS, Guimarães AJ, McCarron P, McCann M et al (2023) Silver(I) 1,10-phenanthroline complexes are active against *Fonsecaea pedrosoi* viability and negatively modulate its potential virulence attributes. J Fungi 9:356. https://doi.org/10.3390/jof9030356
66. Srivastava P, Singleton E, Morrisette T, Berti AD, Ventresca RL, Brassell E et al (2026) The cefazolin inoculum effect: An underappreciated factor in MSSA treatment strategies. Infect Dis Ther 5:417–441. https://doi.org/10.1007/s40121-025-01283-3

67. Sun D, Gao W, Hu H, Zhou S (2022) Why 90% of clinical drug development fails and how to improve it? Acta Pharm Sin B 12:3049–3062. https://doi.org/10.1016/j.apsb.2022.02.002
68. Thomson KS, Moland ES (2001) Cefepime, piperacillin-tazobactam, and the inoculum effect in tests with extended-spectrum β-lactamase-producing Enterobacteriaceae. Antimicrob Agents Chemother 45:3548–3554. https://doi.org/10.1128/AAC.45.12.3548-3554.2001
69. Van Os W, Zeitlinger M (2021) Predicting antimicrobial activity at the target site: Pharmacokinetic/pharmacodynamic indices versus time–kill approaches. Antibiotics 10:1485. https://doi.org/10.3390/antibiotics10121485
70. Vargas-Rigo G, Petro-Silveira B, Devereux M, McCann M, Souza Dos Santos AL, Tasca T (2019) Anti-*Trichomonas vaginalis* activity of 1,10-phenanthroline-5,6-dione-based metallodrugs and synergistic effect with metronidazole. Parasitology 146:1179–1183. https://doi.org/10.1017/S003118201800152X
71. Ventura RF, Galdino ACM, Viganor L, Schuenck RP, Devereux M, McCann M et al (2020) Antimicrobial action of 1,10-phenanthroline-based compounds on carbapenemase-producing *Acinetobacter baumannii* clinical strains: Efficacy against planktonic- and biofilm-growing cells. Braz J Microbiol 51:1703–1710. https://doi.org/10.1007/s42770-020-00351-9
72. Viganor L, Galdino ACM, Nunes APF, Santos KRN, Branquinha MH, Devereux M et al (2016) Anti-*Pseudomonas aeruginosa* activity of 1,10-phenanthroline-based drugs against both planktonic- and biofilm-growing cells. J Antimicrob Chemother 71:128–134. https://doi.org/10.1093/jac/dkv292
73. Viganor L, Howe O, McCarron P, McCann M, Devereux M (2017) The antibacterial activity of metal complexes containing 1,10- phenanthroline: Potential as alternative therapeutics in the era of antibiotic resistance. Curr Top Med Chem 17:1280–1302. https://doi.org/10.2174/1568026616666161003143333
74. WHO. World Health Organization (2017) Prioritization of pathogens to guide discovery, research and development of new antibiotics for drug-resistant bacterial infections, including tuberculosis. World Health Organization, Geneva
75. WHO. World Health Organization (2024) Bacterial priority pathogens list, 2024: bacterial pathogens of public health importance to guide research, development and strategies to prevent and control antimicrobial resistance. World Health Organization, Geneva
76. Yu Y, Rüppel D, Weber W, Derendorf H (2019) PK/PD approaches. In: Vogel HG, Maas J, Gebauer A (eds) Drug discovery and evaluation: methods in clinical pharmacology. Springer, Cham, pp 1–23
77. Zhanel GG, Hoban DJ, Harding GK (1991) The postantibiotic effect: A review of in vitro and in vivo data. Ann Pharmacother 25:153–163. https://doi.org/10.1177/106002809102500210
78. Zhou Y, Hou Z, Fang C, Xue X, Da F, Wang Y et al (2012) Comparison of microplate and macrodilution methods in time–kill study of new antimicrobial drugs. Folia Microbiol 58:9–16. https://doi.org/10.1007/s12223-012-0168-8

# Figures

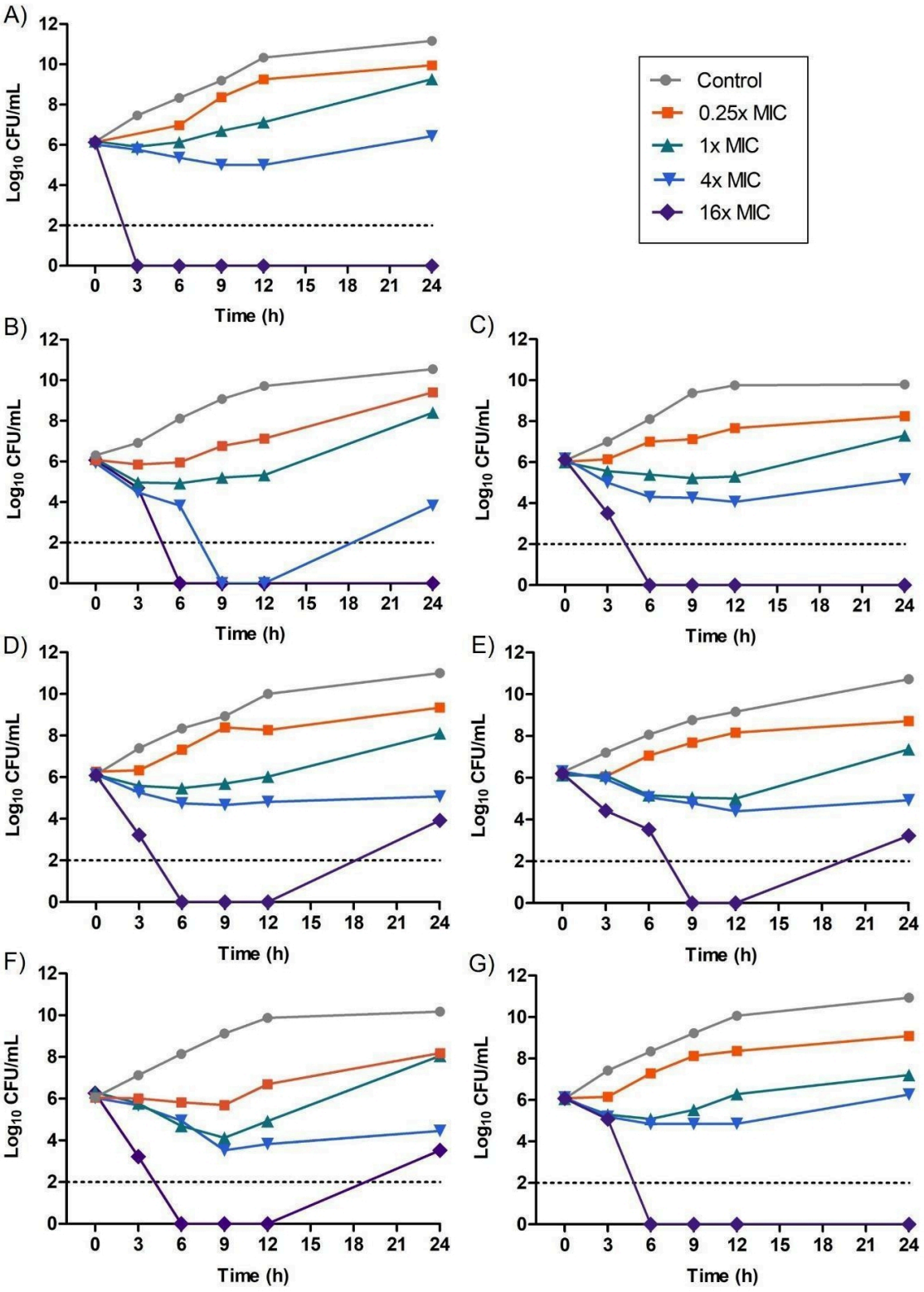



**Figure 1**

Exposure–response curves of seven *A. baumannii* isolates following the treatment with Ag-phendione at 0.25×, 1×, 4×, and 16× the MIC. (a) 3B, (b) 30B, (c) 38B, (d) 78B, (e) 98B, (f) 101B, and (g) ATCC 19606. The dotted line indicates the limit of detection of the method ($10^2$ CFU/mL). Values below this threshold were considered undetectable and reported as no growth.

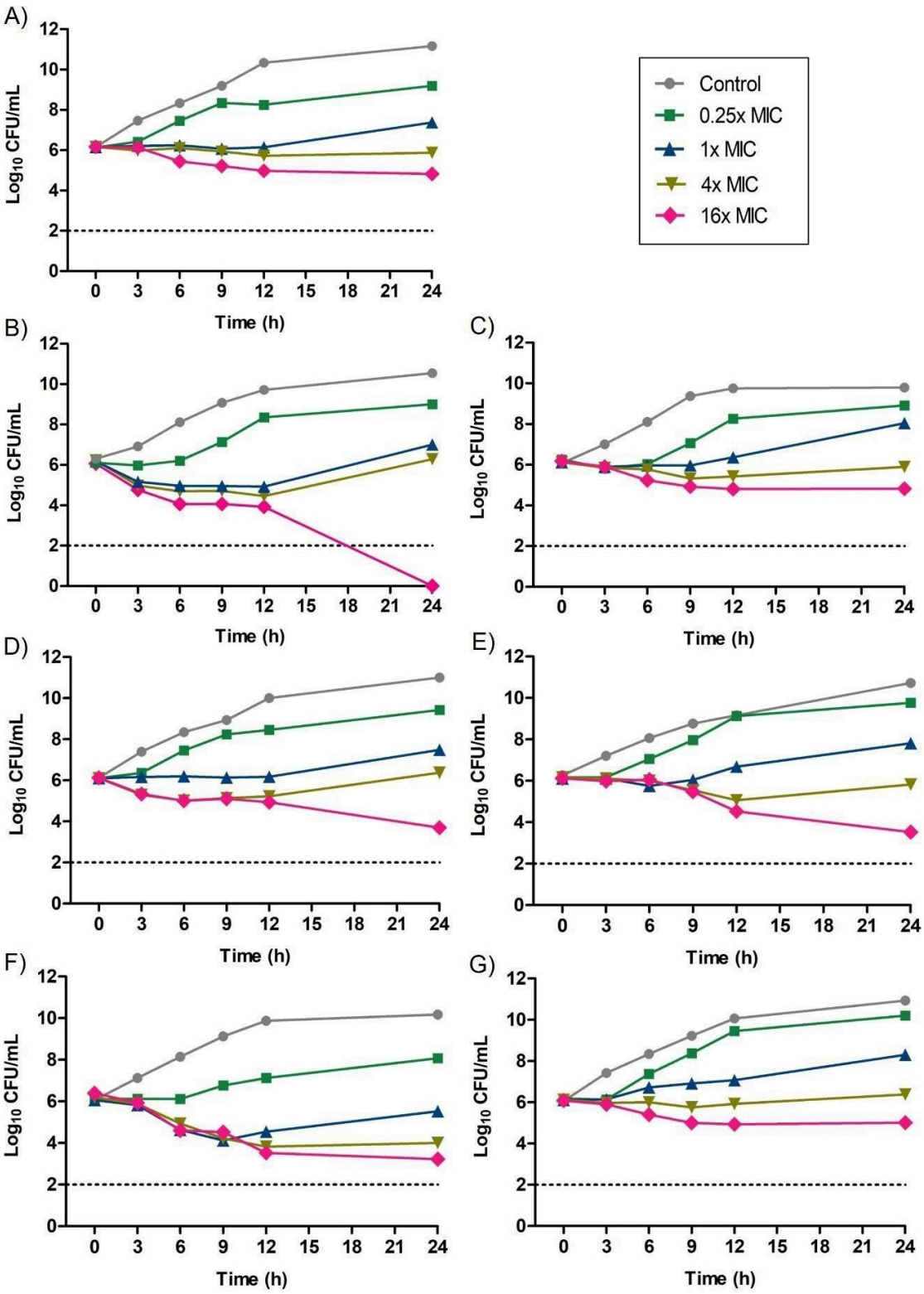



**Figure 2**

Exposure–response curves of seven *A. baumannii* isolates following the treatment with Cu-phendione at 0.25×, 1×, 4×, and 16× the MIC. (a) 3B, (b) 30B, (c) 38B, (d) 78B, (e) 98B, (f) 101B, and (g) ATCC 19606. The dotted line indicates the limit of detection of the method ($10^2$ CFU/mL). Values below this threshold were considered undetectable and reported as no growth.

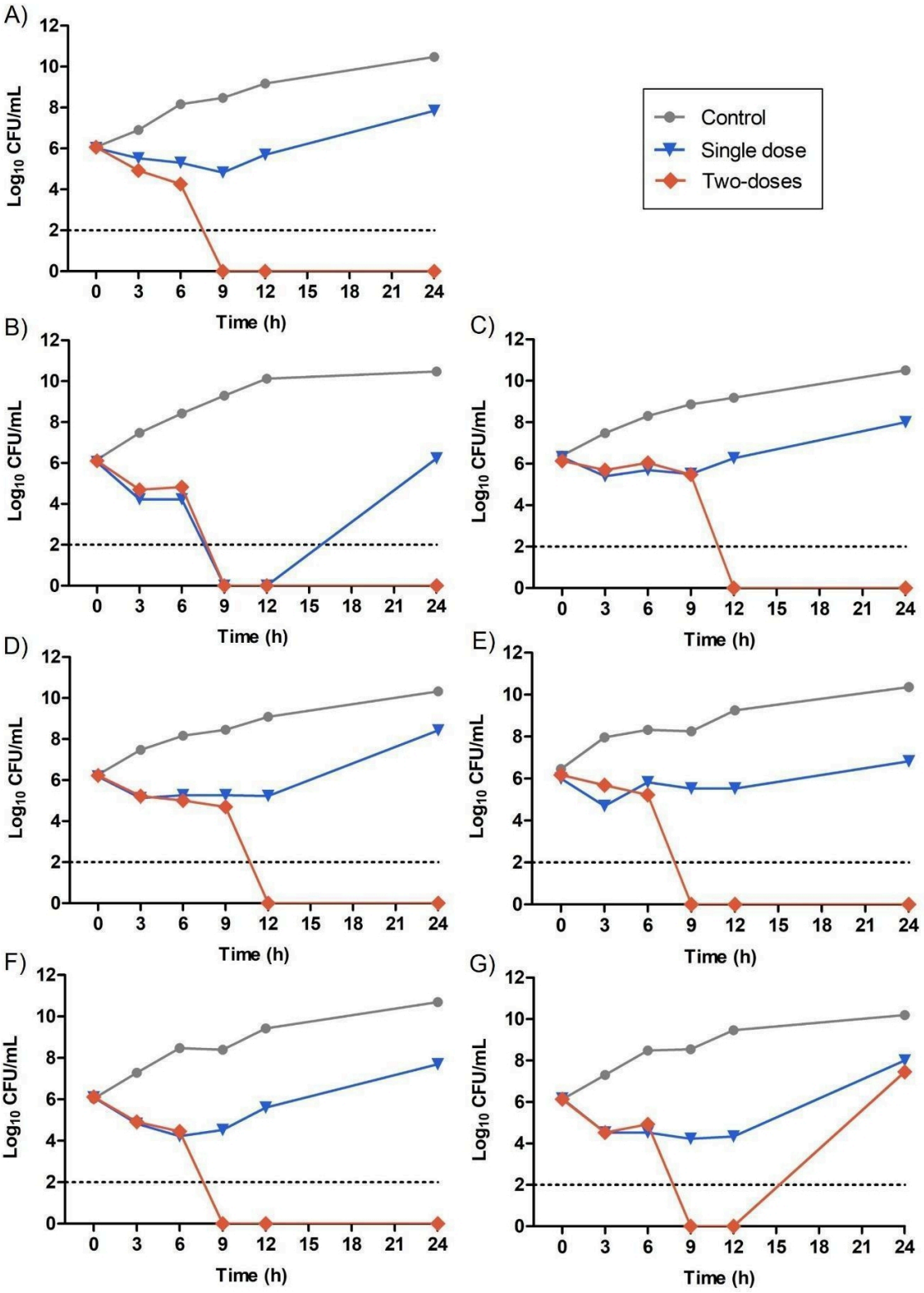



**Figure 3**

Effects of fractionated dosing of Ag-phendione against seven *A. baumannii* isolates. Two sequential doses of Ag-phendione, each corresponding to 0.5× MIC, were administered at 0 and 6 hours. Control groups included an untreated growth control and a single-dose regimen at 1× MIC. (a) 3B, (b) 30B, (c) 38B, (d) 78B, (e) 98B, (f) 101B, and (g) ATCC 19606. The dotted line indicates the limit of detection of the

method (10² CFU/mL). Values below this threshold were considered undetectable and reported as no growth.

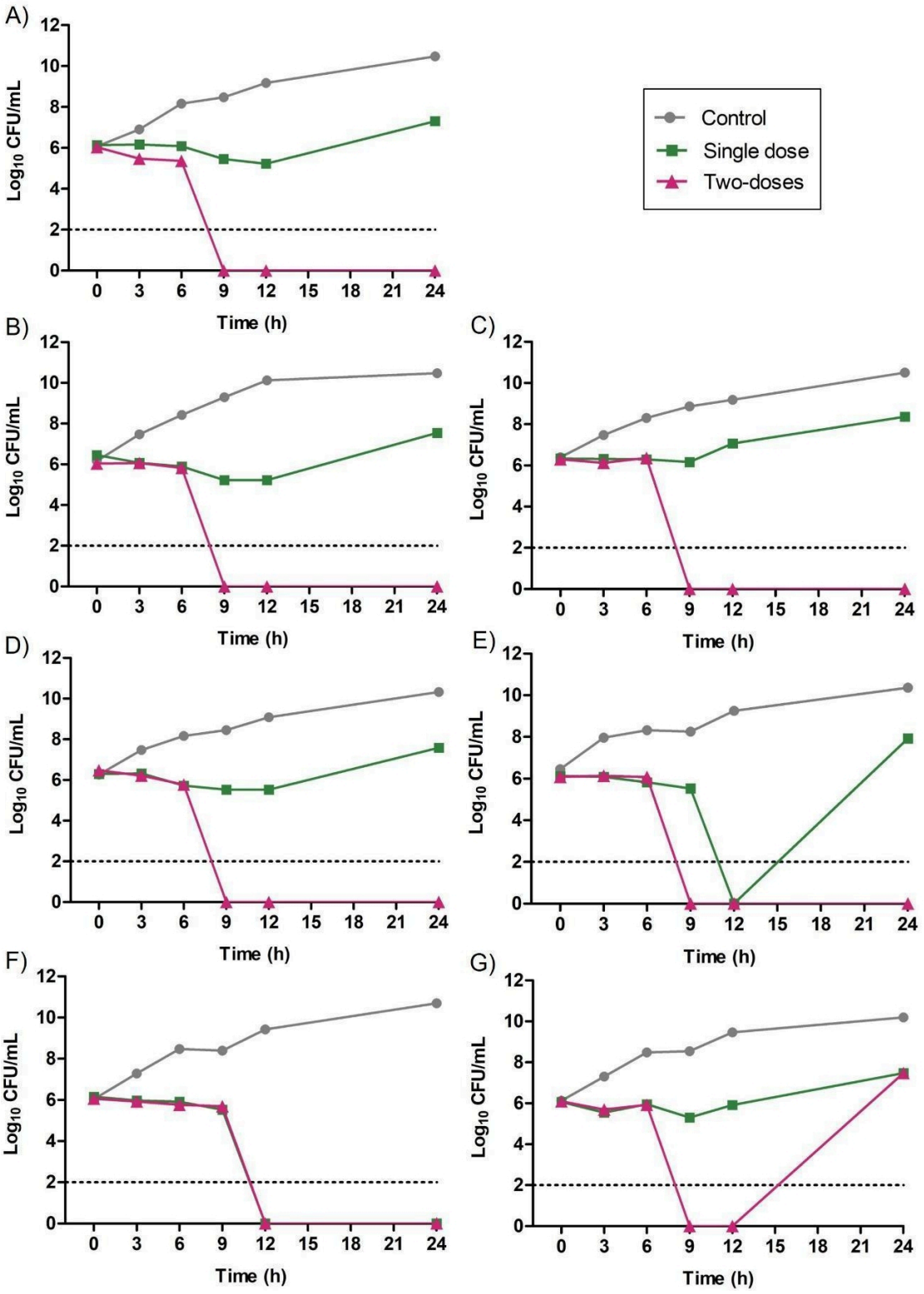



**Figure 4**

Effects of fractionated dosing of Cu-phendione against seven *A. baumannii*isolates. Two sequential doses of Cu-phendione, each corresponding to 0.5× MIC, were administered at 0 and 6 hours. Control

groups included an untreated growth control and a single-dose regimen at 1× MIC. (a) 3B, (b) 30B, (c) 38B, (d) 78B, (e) 98B, (f) 101B, and (g) ATCC 19606. The dotted line indicates the limit of detection of the method (10² CFU/mL). Values below this threshold were considered undetectable and reported as no growth.

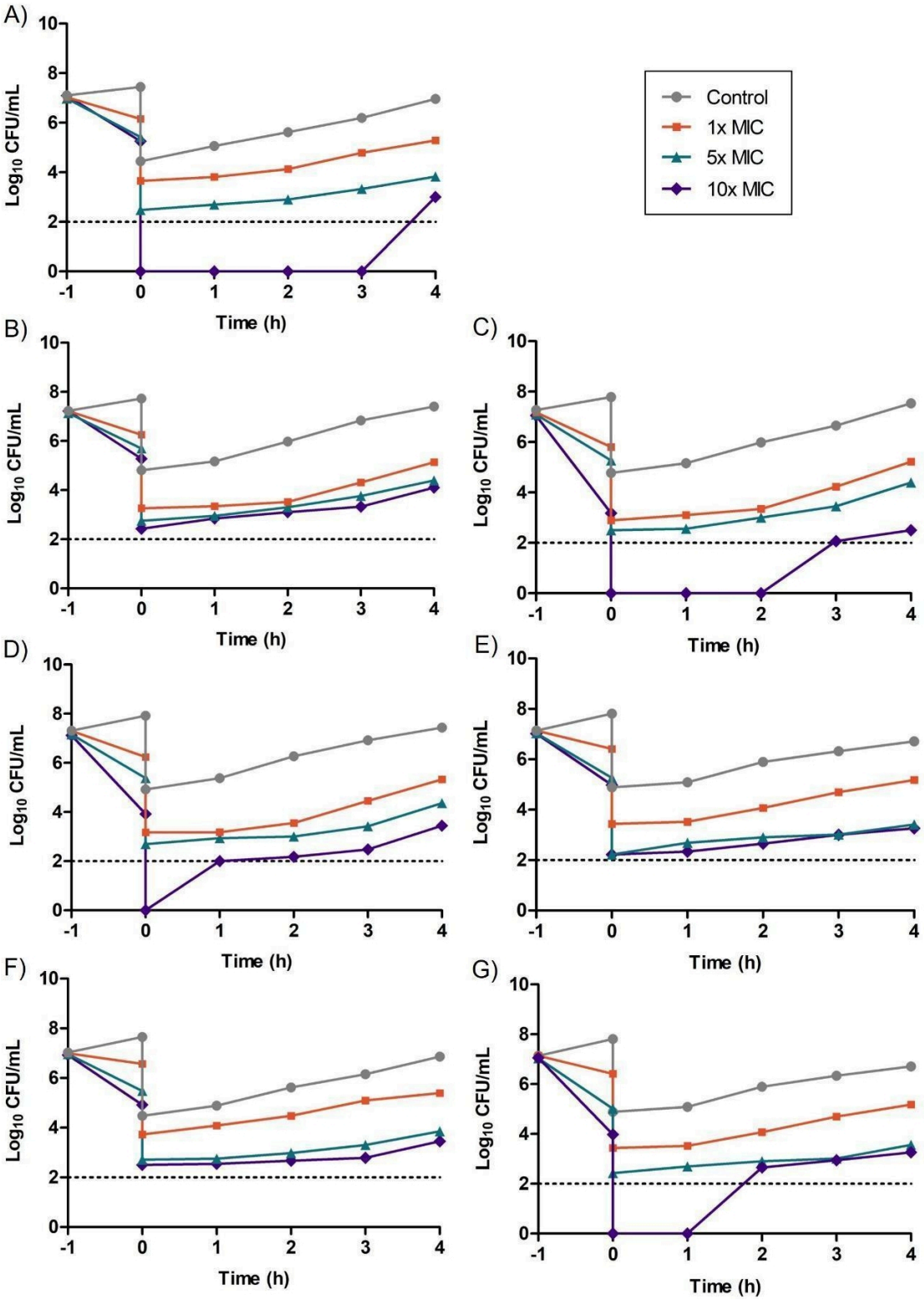



**Figure 5**

Post-antibiotic effect (PAE) induced by a 1-hour exposure to Ag-phendione against seven *A. baumannii* isolates at 1×, 5×, and 10× MIC. At time zero ($T_0$), the compound was removed by a 1:1000 dilution in fresh, drug-free medium, and cultures were subsequently re-incubated. An untreated growth control, processed in parallel without prior exposure to Ag-phendione, was included. (a) 3B, (b) 30B, (c) 38B, (d) 78B, (e) 98B, (f) 101B, and (g) ATCC 19606. The dotted line indicates the limit of detection of the method ($10^2$ CFU/mL). Values below this threshold were considered undetectable and reported as no growth.

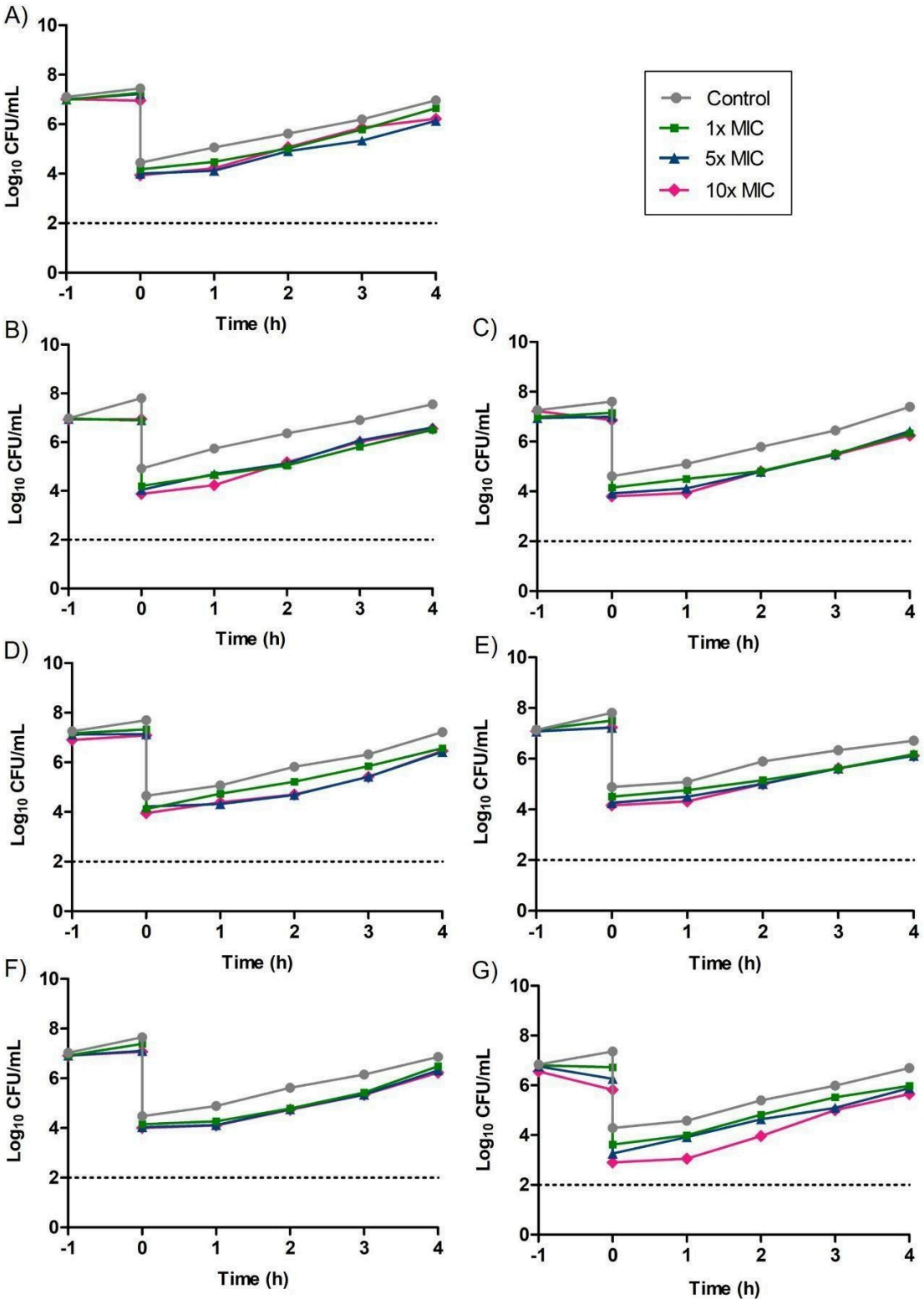


**Figure 6**

Post-antibiotic effect (PAE) induced by a 1-hour exposure to Cu-phendione against seven *A. baumannii* isolates at 1×, 5×, and 10× MIC. At time zero ($T_0$), the compound was removed by a 1:1000 dilution in fresh, drug-free medium, and cultures were subsequently re-incubated. An untreated growth control, processed in parallel without prior exposure to Cu-phendione, was included. (a) 3B, (b) 30B, (c) 38B, (d) 78B, (e) 98B, (f) 101B, and (g) ATCC 19606. The dotted line indicates the limit of detection of the method ($10^2$ CFU/mL). Values below this threshold were considered undetectable and reported as no growth.

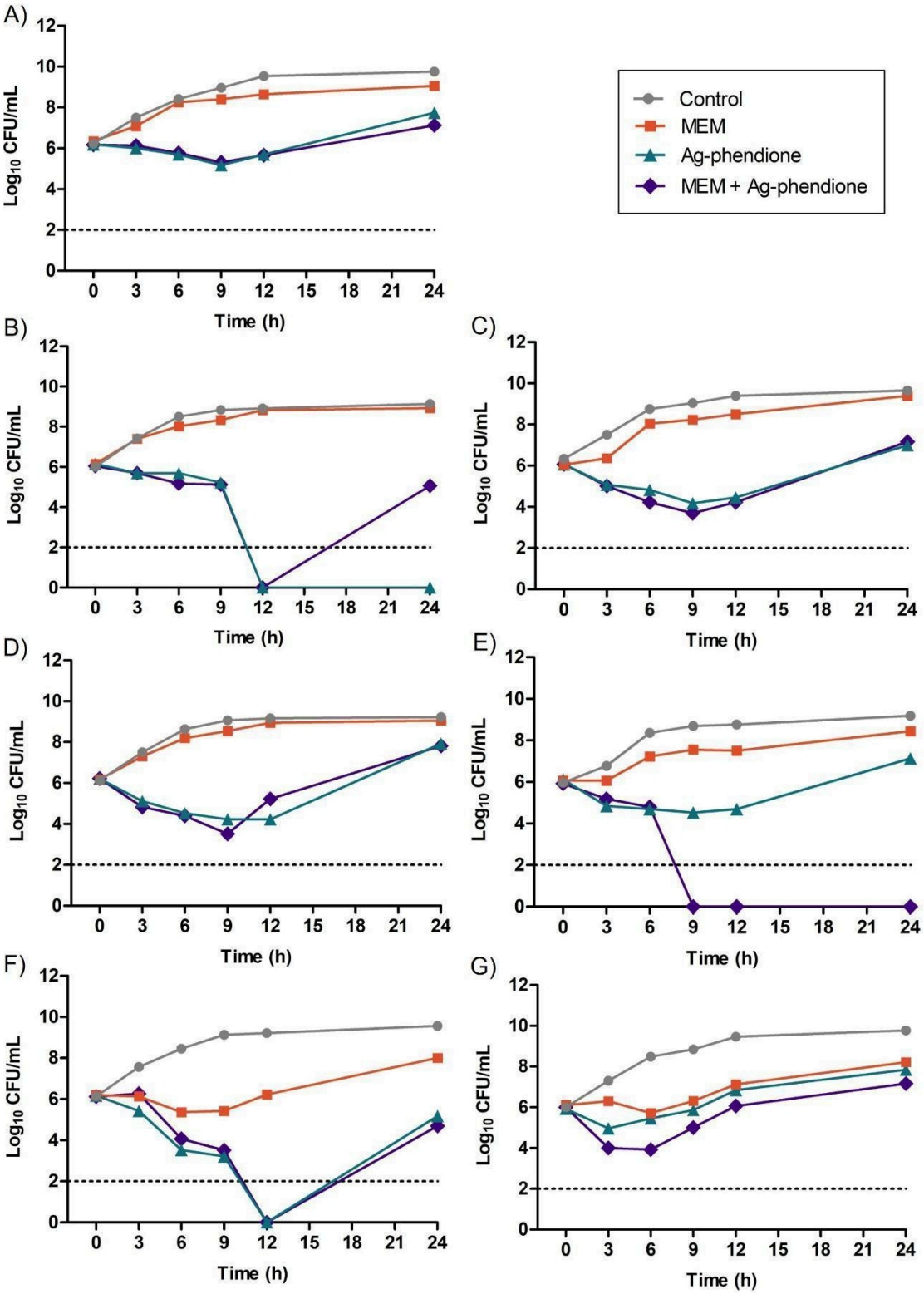



**Figure 7**

**Fig. 8** Time–kill curves of Ag-phendione (0.5× MIC), alone or in combination with meropenem (MEM, 0.5× MIC), against seven *A. baumannii* strains over 24 hours. (a) 3B, (b) 30B, (c) 38B, (d) 78B, (e) 98B, (f) 101B, and (g) ATCC 19606. The dotted line indicates the limit of detection of the method ($10^2$ CFU/mL). Values below this threshold were considered undetectable and reported as no growth.

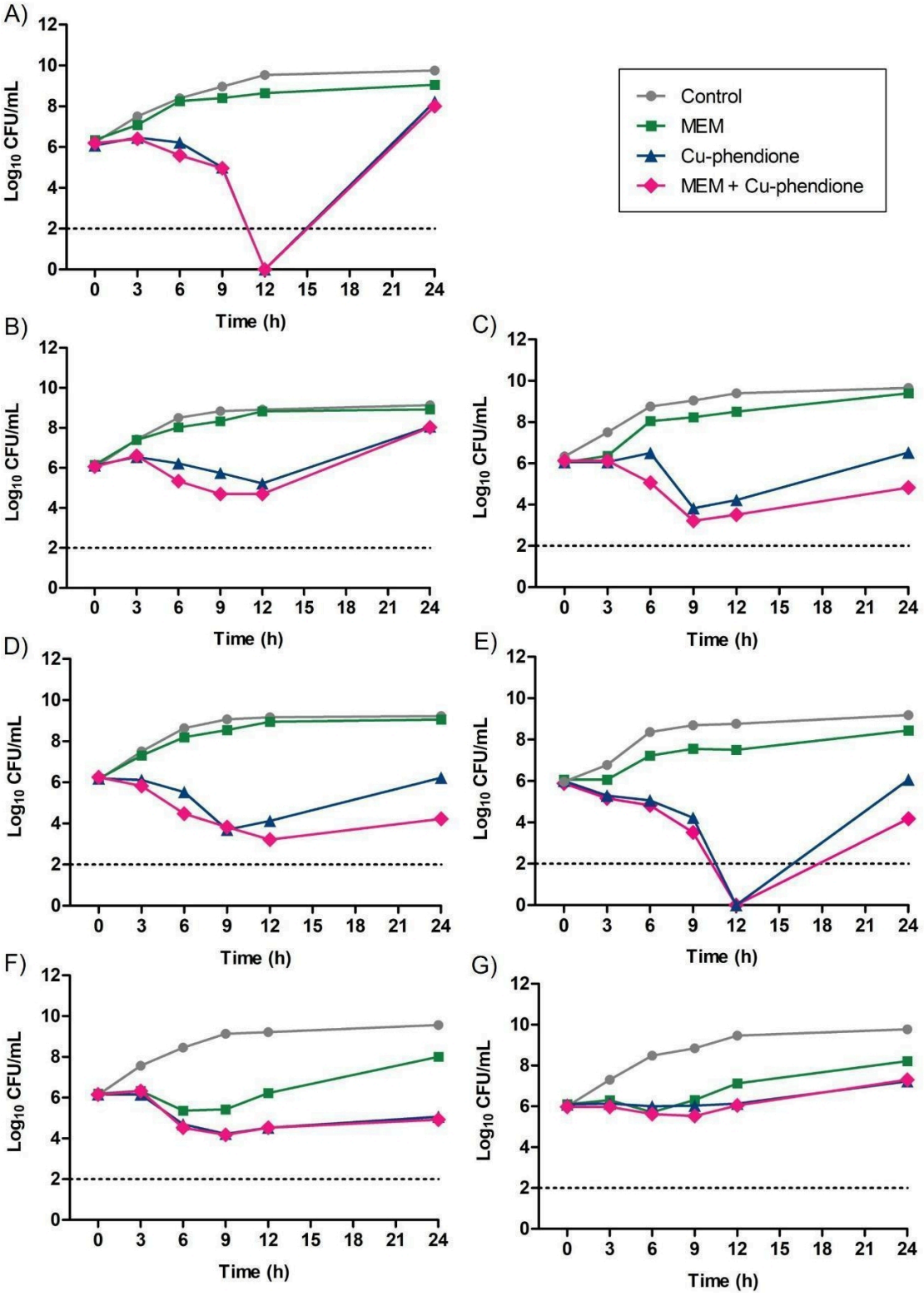



**Figure 8**

**Fig. 9** Time–kill curves of Cu-phendione (0.5× MIC), alone or in combination with meropenem (MEM, 0.5× MIC), against seven *A. baumannii* strains over 24 hours. (a) 3B, (b) 30B, (c) 38B, (d) 78B, (e) 98B, (f) 101B, and (g) ATCC 19606. The dotted line indicates the limit of detection of the method ($10^2$ CFU/mL). Values below this threshold were considered undetectable and reported as no growth.

## Supplementary Files

This is a list of supplementary files associated with this preprint. Click to download.

- PeregrinoSupplementaryInformation.docx